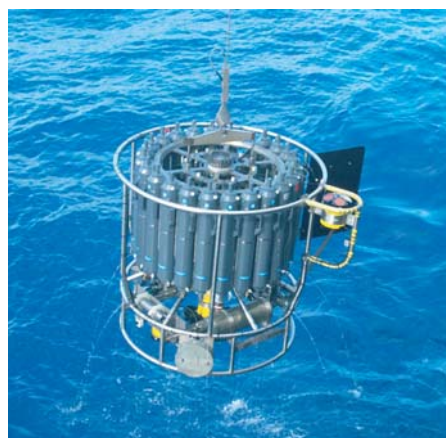




# Single Column Models and Low Cloud Feedbacks

Suvarchal Kumar Cheedela



## Hinweis

Die Berichte zur Erdsystemforschung werden vom Max-Planck-Institut für Meteorologie in Hamburg in unregelmäßiger Abfolge herausgegeben.

Sie enthalten wissenschaftliche und technische Beiträge, inklusive Dissertationen.

Die Beiträge geben nicht notwendigerweise die Auffassung des Instituts wieder.

Die "Berichte zur Erdsystemforschung" führen die vorherigen Reihen "Reports" und "Examensarbeiten" weiter.



## Notice

*The Reports on Earth System Science are published by the Max Planck Institute for Meteorology in Hamburg. They appear in irregular intervals.*

*They contain scientific and technical contributions, including Ph. D. theses.*

*The Reports do not necessarily reflect the opinion of the Institute.*

*The "Reports on Earth System Science" continue the former "Reports" and "Examensarbeiten" of the Max Planck Institute.*

## Anschrift / Address

Max-Planck-Institut für Meteorologie  
Bundesstrasse 53  
20146 Hamburg  
Deutschland

Tel.: +49-(0)40-4 11 73-0  
Fax: +49-(0)40-4 11 73-298  
Web: [www.mpimet.mpg.de](http://www.mpimet.mpg.de)

## Layout:

Bettina Diallo, PR & Grafik

Titelfotos:

vorne:

Christian Klepp - Jochem Marotzke - Christian Klepp

hinten:

Clotilde Dubois - Christian Klepp - Katsumasa Tanaka

# Single Column Models and Low Cloud Feedbacks

Suvarchal Kumar Cheedela

aus Hyderabad, Indien

Hamburg 2014

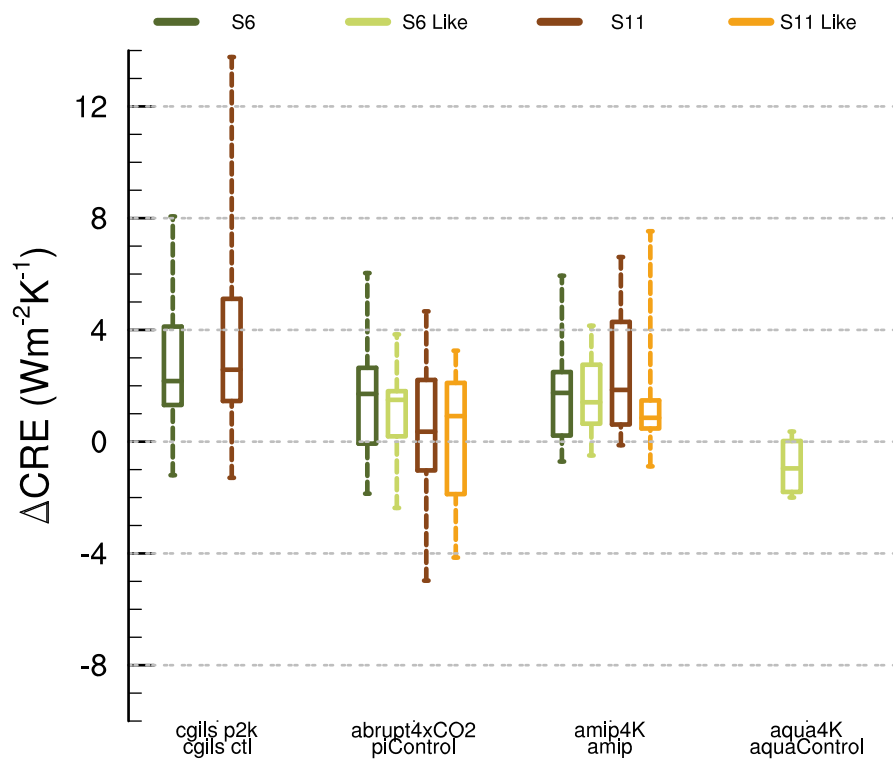
Suvarchal Kumar Cheedela  
Max-Planck-Institut für Meteorologie  
Bundesstrasse 53  
20146 Hamburg

Als Dissertation angenommen  
vom Department Geowissenschaften der Universität Hamburg

auf Grund der Gutachten von  
Prof. Dr. Bjorn Stevens  
und  
Dr. Marco Giorgetta

Hamburg, den 17. Juni 2013  
Prof. Dr. Jürgen Oßenbrügge  
Leiter des Departments für Geowissenschaften

# Single Column Models and Low Cloud Feedbacks



Suvarchal Kumar Cheedela

Hamburg 2013



## Abstract

Low cloud feedbacks are explored using a hierarchy of general circulation model (GCM) configurations. First, the sensitivity of equilibrium solutions of the ECHAM6 Single Column Model (SCM) for two idealized low cloud regimes, stratocumulus and shallow cumulus in the Northeast Pacific is investigated. The results show that an idealized large scale forcing constant in time can produce multiple solutions that are not necessarily representative of solutions with more realistic nature of large scale forcing.

The ability of the SCM to predict changes in low clouds of a GCM is explored across a hierarchy of configurations of the MPI-ESM model family, including fully coupled experiments with abrupt changes in CO<sub>2</sub>, AMIP configurations forced by changes in the sea-surface temperature, and Aquaplanet configurations forced similarly to the AMIP simulations. For these purposes shallow cumulus and stratocumulus regimes are defined based on the large scale state. It is found that the clouds in comprehensive configurations respond differently than in the idealized SCM. The representativeness of the changes in the large-scale environment used in the idealized test case of the SCM is also explored through comparisons with the comprehensive GCM. Although some aspects of changes in large scale environment are captured by the idealized test cases, the changes at the surface and upper troposphere are not well represented. These changes at the surface are possible reasons for the differences between response in GCM and SCM.

The CMIP5 models are more generally evaluated across the hierarchy of configurations to explore the robustness of cloud feedbacks, and the representativeness of the idealized single column forcing. It is found that changes in tropical clouds below 1km, such as stratocumulus and stratus clouds contribute little to inter-model differences in tropical cloud feedbacks.

Various SCMs from an intercomparison performing the same idealized experiments are compared to their comprehensive GCMs in CMIP5. In summary we find that it is difficult to study inter-model differences in low-cloud feedbacks of GCMs using idealized test case for SCMs for at least two reasons. 1) The idealized low cloud regimes considered occur at margins of distributions in most GCM configurations, they do not contribute much to the tropical average and any understanding from them is difficult to transfer to larger regions. 2) Although the changes in large scale environment designed in idealized test case are representative of changes in GCMs to a certain extent, it appears that the cloud feedbacks in the GCM configurations are more sensitive to details of local circulations.





# Contents

<b>1</b>	<b>Introduction</b>	<b>13</b>
1.1	Motivation . . . . .	13
1.2	Hierarchy of Model Configurations . . . . .	14
1.3	Thesis Objective . . . . .	17
1.4	Thesis Outline . . . . .	17
<b>2</b>	<b>Response of a single column model to a stationary large scale forcing</b>	<b>19</b>
2.1	Introduction . . . . .	19
2.2	Experimental framework . . . . .	20
2.3	Single column model under constant large scale forcing . . . . .	24
2.4	Single column model under a stationary, random large scale forcing . . . . .	27
2.5	Conclusions and Outlook . . . . .	35
<b>3</b>	<b>Low-cloud feedbacks in ECHAM6 and CGILS forcing</b>	<b>37</b>
3.1	Introduction . . . . .	37
3.2	Overview of relevant CMIP5 experiments . . . . .	38
3.3	Sorting CGILS and CGILS-like locations . . . . .	42
3.4	Response in CGILS and CGILS-like regions . . . . .	44
3.5	Forcing and Feedback mechanisms at CGILS Locations . . . . .	47
3.6	Conclusions and Outlook . . . . .	54
<b>4</b>	<b>Low-cloud feedbacks in CMIP5 models and single column models in CGILS</b>	<b>55</b>
4.1	Introduction . . . . .	55
4.2	Overview of Cloud Feedbacks in the CMIP5 Models . . . . .	55
4.3	Sorting CGILS Clouds . . . . .	57
4.4	Response in CGILS and CGILS-like areas . . . . .	63
4.5	Conclusions and Outlook . . . . .	66
<b>5</b>	<b>Conclusions</b>	<b>67</b>
	<b>Bibliography</b>	<b>69</b>



# List of Figures

2.1	Initial conditions and large-scale forcing used for the, Stratocumulus (continuous) and Shallow Cumulus (dashed) cases, and for the control (blue) and the perturbed (red) climate. . . . .	23
2.2	Time series (monthly) of simulated cloud cover and liquid water path for the, a) Stratocumulus and b) Shallow Cumulus cases, under a constant large-scale forcing. The grey dots on the vertical axis represent the model vertical grid levels. . . . .	25
2.3	Ensemble time series of liquid water path (monthly) for the, a) Stratocumulus and b) Shallow Cumulus cases, under a constant large-scale forcing. . . . .	26
2.4	Probability Density Function of liquid water path for Shallow Cumulus case under a constant large-scale forcing. The PDFs from the ensemble runs are shown in Black and for the reference simulation in Blue. . . . .	26
2.5	Ensemble time series of Cloud Radiative Effect(monthly) for the, a) Stratocumulus and b) Shallow Cumulus cases, under a constant large-scale forcing. The control case is shown in Blue and the perturbed climate in Red. . . . .	28
2.6	Probability Density Functions (%) of Cloud Radiative Effect for the, a) Stratocumulus and b) Shallow Cumulus cases, under a constant large-scale forcing. The control case is shown in Blue and the perturbed climate case in Red. Bin width is $2 Wm^{-2}$ and the initial months are excluded from the computation. . . . .	29
2.7	Vertical velocity and its standard deviation from the ECMWF reanalysis sampled at a shallow cumulus location in East Pacific, in July 2000. . . . .	30
2.8	Time series (monthly) of simulated cloud cover and liquid water path for the, a) Stratocumulus b) Shallow Cumulus cases under a random large scale forcing. The random forcing applied is 50% of mean vertical velocity and introduced every 6 hours. The Grey dots on the vertical axis indicate the model vertical grid levels. . . . .	31

LIST OF FIGURES

2.9 Ensemble time series of liquid water path(monthly) for the, a) Stratocumulus b) Shallow Cumulus cases, under a random large-scale forcing. The magnitude of large scale forcing applied is 50% of the mean vertical velocity and introduced every 6 hours. . . . . 31

2.10 Probability Density Function (%) of liquid water path for the Shallow Cumulus cases under random large-scale forcing, with magnitude a) 50 % of mean, introduced every 6 hours and b) 20 % of mean, introduced every 6 hours. The PDFs from the ensemble runs are shown in Grey and for the reference simulation in Blue. . . . . 32

2.11 Ensemble time series of Cloud Radiative Effect(monthly) for the, a) Stratocumulus and b) Shallow Cumulus cases, under a random large-scale forcing. The control climate is shown in Blue and the perturbed climate case in Red. The magnitude of large scale forcing applied is 50% of the mean vertical velocity and introduced every 6 hours. . . . . 32

2.12 Probability Density Functions (%) of Cloud Radiative Effect for the, a) Stratocumulus and b) Shallow Cumulus cases under a random large-scale forcing. The control climate is shown in Blue and the perturbed climate case in Red. The magnitude of large scale forcing applied is 50% of the mean vertical velocity and introduced every 6 hours. Bin width is  $2 Wm^{-2}$  and the initial months are excluded from the computation. . . . . 33

2.13 Change in Cloud Radiative Effect ( $Wm^{-2}$ ) for the, a) Stratocumulus and b) Shallow Cumulus cases under a random large-scale forcing of varying magnitude but same mean. The vertical axis represents the magnitude of large scale forcing applied, (% of the mean vertical velocity) and the horizontal axis represents frequency over which the forcing is used. Hatched regions are the locations where the change in Cloud Radiative Effect is uncertain. . . . . 34

3.1 Annually averaged change in Cloud Radiative Effect( $Wm^{-2}$ ) for the selected CMIP5 experiment sets. CGILS, Stratocumulus and Shallow Cumulus locations are indicated by a circle and square. CGILS-like Stratocumulus and Shallow Cumulus locations are indicated by lines and dots. Summer-like points are indicated by darker dots and lines. . . . . 41

LIST OF FIGURES

3.2 Average cloud top height sorted based on omega at 500hPa and LTS. Joint distribution of omega and LTS are showed by black contour lines with 1% intervals. CGILS-like Stratocumulus and Shallow Cumulus locations, are indicated by shaded regions with lines and dots respectively. . . . . 43

3.3  $\Delta$ Cloud Radiative Effect( $Wm^{-2}K^{-1}$ ) per degree of surface temperature change, during boreal summer in the selected CMIP5 experiments. CGILS-like Stratocumulus and Shallow Cumulus regions are hatched with lines and dots. . . . . 45

3.4 Cloud feedbacks ( $Wm^{-2}K^{-1}$ ) at CGILS and CGILS-like locations for the selected heirarchy of configurations. . . . . 46

3.5 Percentage changes in largescale state at CGILS and CGILS-like locations, in the selected heirarchy of model configurations. The values indicated for CGILS single column are based on initial profiles of experimental design. . . . . 48

3.6 Percentage changes in surface fluxes at CGILS and CGILS-like locations, in the selected heirarchy of model configurations. The values indicated for CGILS single column are based on the equilibrium simulations by using single column model. . . . . 49

3.7 Percent changes in total cloud cover (upper) and liquid water path (middle) and absoute changes in cloud top height (hPa, bottom) , in the GCM configurations.CGILS-like Stratocumulus and Shallow Cumulus regions are hatched with lines and dots. . . . . 51

3.8 Percent changes in upward sensible heat flux (upper), upward latent heat flux (middle) in the selected GCM configurations.CGILS-like Stratocumulus and Shallow Cumulus regions are hatched with lines and dots. . . . . 52

3.9 Percent changes in: vertical integrated relative humidity over 800hPa-1000hPa(upper); 500hPa-700hPa (bottom) .CGILS-like Stratocumulus and Shallow Cumulus regions are hatched with lines and dots. . . . . 53

3.10 Percent changes in precipitation in selected heirarchy of GCMs.CGILS-like Stratocumulus and Shallow Cumulus regions are hatched with lines and dots. . . . . 53

4.1 Table of CMIP5 models used . . . . . 56

4.2 Rank correlation of tropical averaged CRE, for coupled models vs. amip models on the left and amip models vs. aquaplanets on the right. . . . . 57

LIST OF FIGURES

4.3	JJA average cloud top height (hPa) sorted based on omega at 500hPa and LTS. Joint distribution of omega and LTS are showed by black contour lines with 1% contour intervals. CGILS-like Stratocumulus and Shallow Cumulus locations, are indicated by shaded regions with lines and dots respectively. . . . .	59
4.4	JJA average change in Cloud Radiative Effect( $Wm^{-2}$ ) sorted on large scale vertical velocity and lower tropospheric stability. Joint distribution of omega and LTS are showed by black contour lines with 1% contour intervals. CGILS-like Stratocumulus and Shallow Cumulus locations, are indicated by shaded regions with lines and dots respectively. . . . .	60
4.5	JJA average change in Cloud Radiative Effect( $Wm^{-2}$ ) sorted on large scale vertical velocity and lower tropospheric stability. Joint distribution of omega and LTS are showed by black contour lines with 1% contour intervals. CGILS-like Stratocumulus and Shallow Cumulus locations, are indicated by shaded regions with lines and dots respectively. . . . .	61
4.6	Rank correlation of CRE per degree of surface temperature change for coupled models vs. amip models. . . . .	62
4.7	(a) Change in Cloud Radiative Effect( $Wm^{-2}$ ) b) Percentage change in LTS c) HYL and d) Omega at 500hPa, per degree of surface temperature change for CGILS and CGILS like locations. Quartile range from CGILS constant forcing is also indicated in Black . . . . .	64
4.8	Rank correlation of CRE per degree of surface temperature change for coupled models vs. single column models. . . . .	65

# List of Tables

2.1	Large scale conditions for the experiments . . . . .	21
3.1	Overview of MPI-ESM-LR CMIP5 experiments: Number of years considered, change in SST and CRE over tropical (40S to 40N) oceans . . . . .	39
3.2	Overview of CGILS and CGILS-like locations . . . . .	43
3.3	Changes in 700hPa downward radiative fluxes ( $Wm^{-2}$ ) in amip configuration: downward longwave radiation (RLD), clear-sky downward longwave radiation (RLDCS), upward longwave radiation (RLU), clear-sky upward longwave radiation (RLD), downward shortwave radiation (RSD), clear-sky downward shortwave radiation (RSDCS), upward shortwave radiation (RSD), and clear-sky upward shortwave radiation (RLD) . . . . .	50





# Chapter 1

## Introduction

### 1.1 Motivation

Clouds play a key role in the energy balance of the Earth. Clouds modify the incoming shortwave radiation (albedo) and outgoing thermal longwave radiation (greenhouse effect) of the Earth. They are an important part of the hydrological cycle. Along with the radiative effects, the latent heating during the cloud formation modifies the atmospheric circulations. Yet the role of clouds in large scale atmospheric circulations is poorly understood and remains a grand challenge in atmospheric science. Hence the response of clouds to a climate perturbation, for instance, a warming under doubling of CO<sub>2</sub> remains elusive. Cloud feedbacks are main cause for inter-model differences in model-based estimates of climate sensitivity (Soden and Held 2006).

Although the importance of clouds feedbacks in climate is long recognized (e.g., Arakawa (1975)), they remain difficult to understand because of the coarse resolution and the assumptions that underlie the parametrizations in current climate models. Given the shallow depths and ubiquitous extent of low clouds, it is not surprising that most uncertainty in cloud feedbacks comes from low clouds (Bony 2005; Bony et al. 2006; Webb et al. 2006). Their proximity to surface leads to a relatively warm cloud top. Hence they do not alter the effective emissivity of the atmosphere, contributing more to the cooling effect of the planet. Thus predicting changes in these clouds is important for the climate sensitivity. It is often easy to show that a high climate sensitivity model is associated with strong positive low cloud feedback and a low climate sensitivity model is associated with a strong negative cloud feedback (Stephens 2005).

Any changes in clouds are strongly coupled to changes in large scale circulations. It is this strong interaction, that makes it hard to identify the leading causes for differences in the cloud feedbacks among the comprehensive climate models. The complexity of cloud feedbacks mandates use of simplified configurations such as atmosphere-only, aquaplanets, and single column models. Although

## 1. INTRODUCTION

these simplified configurations help to identify different aspects of the problem, it is still not clear to what extent these configurations act as analogs to study the response of low-clouds in full complexity, coupled model.

The goal of the thesis is to identify the extent to which above mentioned frequently used simplified configurations can be used to predict the cloud feedbacks of comprehensive, coupled configuration. The focus is on low cloud feedbacks at select locations in the Northeast Pacific. With increasing model intercomparisons such as Coupled Model Intercomparison Project 5 (CMIP5), it is now possible to answer this question in general which otherwise was limited by the individual models. This study help us to better understand the inter-model differences in low cloud feedbacks and further exploit the relative simplicity of configurations in synergy.

## 1.2 Hierarchy of Model Configurations

In this section we present an overview of the model configurations used in the study. The model configurations are presented in the order of complexity.

### 1.2.1 Coupled models

A coupled atmospheric-ocean-land model is the most comprehensive general circulation model (GCM) configuration representing of our best understanding of earth system and its processes relevant for climate. This configuration is computationally very intensive due to the number of processes and long adjustment timescales between its components. Standardized experiments using this configuration are used to asses progress in our understanding of climate change (e.g, Solomon et al. (2007)). CMIP5, is recent activity with standardized climate change experiments (Taylor et al. 2012) using contemporary climate models. The results from this activity are used to asses the current understanding of climate and climate change by the ongoing Intergovernmental Panel for Climate Change.

The challenge is to understand the response of such a model to a climate perturbation. The complexity of the coupled model makes it hard to understand the changes in clouds in midst of other changes. An aim of the simplified configurations is to understand different aspects of a coupled model. The experiments from CMIP5 with unprecedented number of output diagnostics and simplified model configurations presents an opportunity for rapid progress in understanding the cloud feedbacks.

### 1.2.2 AMIP

A GCM configuration without an ocean component, instead prescribed by Sea Surface Temperature (SST) at the boundary, is frequently referred as atmospheric GCM or atmosphere-only model. This configuration is convenient framework to understand aspects of atmospheric circulations at much faster adjustment timescales. It is the most preferred configuration for the development of the atmospheric models. The Atmospheric Model Intercomparison Project (AMIP, Gates et al. (1999)) was initiated in an effort to understand biases in atmospheric components of comprehensive GCMs. In AMIP, the models are prescribed by observed SST, referred as AMIP SST and observed sea-ice concentrations. Eventually, the name AMIP has become synonymous to atmosphere-only model prescribed by observed SST.

Often the large scale atmospheric circulations in AMIP and Coupled configurations are similar. Cess et al. 1990 proposed experiments using Atmospheric GCMs by uniform increase in SST as a surrogate to understand the climate sensitivity of coupled models. They found that the climate sensitivity of majority of atmospheric models of that time are similar to their coupled counterparts. In such studies often global or tropical averages are used, it would be interesting to know the details to which the cloud feedbacks in the configurations are similar. The experiments in CMIP5 performed using AMIP, can help us to dwell into similarities and differences in cloud feedbacks of AMIP models to the coupled model.

### 1.2.3 Aquaplanets

Aquaplanet is a configuration of atmospheric-only GCM free from land. Often Aquaplanets are prescribed by zonally symmetric SSTs that vary only with latitude, there is no sea ice, and no seasonal changes in insolation. Because of their relative simplicity they have been used in various contexts, for instance to study tropical intra-seasonal oscillations (e.g, Goswami and Shukla (1984), Hayashi and Sumi (1986)). Aquaplanets are also useful for exploring other aspects of atmospheric circulation, for instance the relative role of zonally symmetric versus asymmetric circulations. With recent studies using aquaplanets such as Medeiros et al. (2008), Medeiros and Stevens (2011), there is growing interest in using aquaplanets to understand the aspects of low-clouds and their interactions with large scale circulations. Medeiros et al. (2008) showed that the tropical sensitivity of aquaplanets is similar to that of AMIP configurations using two different models. In a further study Medeiros and Stevens (2011) using four models they showed aquaplanets captured core of distribution of AMIP configurations. With CMIP5

## 1. INTRODUCTION

also featuring experiments using aquaplanets, the cloud feedbacks can now be studied across the hierarchy of GCM configurations, including the aquaplanets of several models.

### 1.2.4 Single Column Models

A single column model (SCM) is an isolated column of a atmosphere-only GCM with all its parametrizations for the unresolved scales. A single column model can be prescribed by the resolved large-scale circulation, thereby it becomes a natural framework to test and develop the parametrizations by comparing to the point observations or high resolution models. Although SCMs were used from early studies of parametrizations (e.g, Betts and Miller (1986)), GEWEX Cloud System Study (GCSS, Browning et al. (1993)) community through various SCM intercomparisons has popularized use of SCMs as tools to improve representations of clouds. The key advantage of a SCM is its ability to show the processes in detail and at a minimal computational expense.

Zhang and Bretherton (2008) and Zhang et al. (2012) in coordination with Cloud Feedback Model Intercomparison Project (CFMIP) group proposed an intercomparison of contemporary SCMs using idealized climate change experiments representative of select low cloud locations in Northeast Pacific. This intercomparison is referred here onwards as CFMIP-GCSS Intercomparison of Single column and Large-eddy Simulations (CGILS). The aim is to exploit the advantages of single column model and to understand the mechanisms causing inter-model differences in low-cloud feedbacks and evaluate these mechanisms using fine resolution large-eddy simulations.

This intercomparison uses a set of idealized large scale forcings designed to represent the changes in the local environment of subtropical clouds in a warmer climate at three low-cloud locations in Northeast Pacific. We use two locations representative of Stratocumulus and Shallow cumulus. The utility of such experiments depends on whether or not idealized SCM experiments can reproduce the different feedbacks seen in the comprehensive configurations. This further depends on the extent to which CGILS large scale forcing captures the aspects of comprehensive GCMs.

Evaluating changes in largescale forcing of CGILS is also interesting because it encompasses some of current conceptual understanding of large scale circulations. Much of current understand of role of clouds in climate is due to conceptual models (e.g, Pierrehumbert (1995), Miller (1997), Larson et al. (1999)). Drawing connections between simple model configurations and the comprehensive GCMs would help to better understand and assess the role of clouds in the climate. It is because of these aspects that makes single column models a focus of the thesis.

## 1.3 Thesis Objective

- To assess the ability of idealized single column model experiments to predict the low-cloud feedbacks in the GCMs.
- To evaluate CMIP5 models across the hierarchy of configurations to explore the robustness of cloud feedbacks.

## 1.4 Thesis Outline

- Chapter 2: In this Chapter 2 we introduce CGILS idealized climate change experiments for the single column models. We explore the sensitivity of equilibrium solutions of MPI-ESM-LR single column model to the nature of largescale forcing used.
- Chapter 3: In Chapter 3 we present the relevant strategy to compare cloud feedbacks across hierarchy of MPI-ESM-LR model configurations. We compare the cloud feedbacks and changes in large scale forcing at CGILS and similar locations. Possible causes for low cloud feedbacks and differences between the model configurations are presented.
- Chapter 4: In Chapter 4 we evaluate robustness of cloud feedbacks in CMIP5 models across the GCM model hierarchy. Using the strategy outlined in Chapter 3, we compare cloud feedback from the single column models of CGILS intercomparison to the CMIP5 GCM configurations, to assess the ability of CGILS to predict low cloud changes of GCM. The representativeness of CGILS idealized climate change in GCMs is evaluated.
- Chapter 5: In this Chapter we present the conclusions and outlook from the thesis.



## Chapter 2

# Response of a single column model to a stationary large scale forcing

### 2.1 Introduction

Despite the improvements in representation of cloud processes in various climate models, the response of the boundary layer clouds under the climate change remains uncertain. These low-cloud feedbacks currently pose a challenge for constraining the climate sensitivity, with a disagreement even in the sign of low-cloud feedbacks among different GCMs (eg. Bony (2005); Stephens (2005)). In view of these difficulties, Zhang et al. (2009) proposed an idealistic climate change experiment for a single column model over selective low cloud conditions, in an aim to understand the physical mechanisms involving the low-cloud feedbacks. This was later turned into an intercomparison of various single column models, called CFMIP-GCSS Intercomparison of Large-Eddy and Single-Column Models (CGILS Intercomparison), A simultaneous intercomparison of large-eddy models for the idealized climate change will provide physical mechanisms for evaluating the single column models. The experimental conditions, the derivation of the CGILS large-scale forcing and the idealistic climate change at the Stratocumulus and Shallow Cumulus locations are described in the section 2.2.

A single column model does not allow feedback to the large scale flow and permits additional degrees of freedom in imposing the large-scale forcing as compared to the three dimensional GCM. These aspects can make it hard to translate the results of a single column model to a GCM. The goal of the study is to understand such aspects in ECHAM6 single column model and the consequences to CGILS intercomparison.

In the CGILS intercomparison, a single column model is run to equilibrium under a control climate and a perturbed climate and the difference between the two equilibrium simulations is analyzed for the cloud feedback. An underlying assumption of such analysis is that, a single equilibrium solution of a single column

## 2. RESPONSE OF A SINGLE COLUMN MODEL TO A STATIONARY LARGE SCALE FORCING

model is representative. Hack et al. (2000) found the ensembles (perturbed initial conditions) of their single column model diverge during a 10 day forecast and recommend an additional relaxation term in the single column models to make the solutions representative. However, they also noted a presence of a strong restoring force in their single column model, that brought the ensembles closer at the end of the 10 day forecast. It is not clear, what could happen to the ensembles when the model is further run to an equilibrium. The lack of feedback to the large scale flow in a single column model can lead to multiple locked equilibrium states and using a constant large-scale forcing in time does not mimic any such feedback. The behavior of ECHAM6 single column model under a constant large-scale forcing is explored in Section 2.3. The cloud feedback simulated under such constant large-scale forcing and subject to the CGILS climate change is described in Section 2.3.1.

Furthermore, in a related study, Brient and Bony (2012) found it difficult to compare the cloud fraction from their single column model under a constant large scale forcing to that of their GCM cloud fraction, sampled at similar conditions. A better comparison of cloud fraction was achieved when a random, stationary large-scale forcing is used. They hypothesised this was due to the discrete representation of convection in their model, a time varying large scale forcing was needed to mimic the alternating deep convection, shallow convection and no convection of their GCM. Such time varying large-scale forcing is generated automatically in a three-dimensional GCM, where as a single column model has the additional degrees of freedom in imposing the large scale forcing. Using a random, stationary large scale forcing in time has an additional advantage that it can mimic the large scale feedback in the single column model. The behavior of ECHAM6 single column model under a random, stationary large scale forcing is explored in Section 2.4. However, the degree of randomness is not obvious, the cloud feedbacks simulated under different stationary, random large scale forcing is described in Section 2.4.1.

The conclusions and outlook of the study are presented in Section 2.5.

## 2.2 Experimental framework

The derivation of the large scale forcing for the CGILS control and perturbed climate follows Zhang et al. (2009, 2012). For clarity, the derivation is summarized here.

The CGILS forcing is constructed along a transect in the pacific from the coast of California to Hawaii(GPCI crossection, Teixeira et al. (2011)). Although the large-scale forcing for the control and perturbed climate are constructed all along



Table 2.1: Large scale conditions for the experiments

Conditions	Stratocumulus	Shallow Cumulus
Latitude	32N	17N
Longitude	129W	149W
Time	july	july
Insolation(TOA)	471.5	448.1
SST(C)	19.3	25.6

the transect, only three locations are used for CGILS intercomparison, the Stratus case, the Stratocumulus case and the Shallow Cumulus case. Here, in this study only two of them are used, the Stratocumulus case and the Shallow Cumulus case.

Table 2.1 summarizes the large scale conditions for Stratocumulus and Shallow Cumulus cases. Both the cases are representative of summer, the Stratocumulus case lies on much cooler sea surface temperatures than the Shallow Cumulus case, indicating a shallower boundary layer.

*The control climate:* The temperature, specific humidity, winds, surface temperature and pressure are prescribed from the year 2006 of ECMWF reanalysis at all the locations along the transect. The control climate temperature and specific humidity at the Stratocumulus and Shallow Cumulus locations are shown in Figure 2.1. For deriving the large scale forcing ( $\omega$  and horizontal advection tendency), the basic strategy is to derive the large scale forcing at 35N and extend it to other locations by a fixed set of scaling factors, estimated from the ECMWF reanalysis.

At 35N, the modified weak temperature gradient approximation is used to derive the large scale forcing (Equation 2.1). Firstly, the clear sky radiative fluxes are calculated by using the Rapid Radiative Transfer Model. A profile of  $\omega$ , which peaks at 800hPa is assumed, equation 2.2. Now, to find the amplitude of  $\omega$ , the Equation 2.1 is integrated from 300hPa to 900hPa. The vertical integrated horizontal advection tendency is estimated from ECMWF reanalysis as 2.3K/s at 35N, when substituted gives the amplitude of  $\omega$  profile. Re-substituting back in the original Equation 2.1, gives vertical distribution of horizontal advection tendency. Although this procedure can be followed at all the other latitudes a simpler approach is taken, scaling the large scale forcing according to a set of scaling weights derived from the ECMWF reanalysis. This alienates the necessity to calculate the vertical integrated horizontal advection tendency from ECMWF reanalysis at all the locations and moreover the modified weak temperature gradient

## 2. RESPONSE OF A SINGLE COLUMN MODEL TO A STATIONARY LARGE SCALE FORCING

approximation equation is weaker as we move towards lower latitudes.

$$\frac{\partial T}{\partial t}_{Clear-Skyradiation} = \omega \frac{\partial T}{\partial p} + \left(\frac{\partial T}{\partial t}\right)_{Hadvection} \quad (2.1)$$

$$\omega(p) = \begin{cases} A \cos\left[\frac{(p-100)}{(p_{max}-100)} \times \frac{\pi}{180}\right] & \text{for } 100hPa < p < 800hPa \end{cases} \quad (2.2)$$

At the surface, the surface temperature and horizontal winds are used to calculate the horizontal advection tendency at all the locations. Here again the winds are taken from ECMWF reanalysis. The surface tendencies are kept constant till 950hPa and linearly interpolated to the values at 850hPa. The resulting large scale forcing for the stratocumulus and shallow cumulus locations are shown in Figure 2.1.

*The perturbed climate:* An important aspect for deriving the forcing for the perturbed climate is the derivation of temperature profile. The surface temperature is increased by 2K, at the other heights the temperature of control is incremented such that the gradient in equivalent potential temperature remains same as the control. This is achieved by the following procedure; from the surface to the lifting condensation level (LCL) the control temperature is increased by 2K. Above LCL, at each height, undiluted parcels are brought along moist-adiabat to LCL pressure, this gives a temperature, this temperature is incremented by 2K and followed back moist-adiabatically to initial pressure to give the perturbed climate temperature profile. The relative humidity of the control climate is maintained, this gives the profile of specific humidity. The perturbed climate temperature and specific humidity at the Stratocumulus and Shallow Cumulus locations are shown in Figure 2.1. Due to change in the slope of moist adiabat with changes in temperature, lower tropospheric stability in Stratocumulus cases increases by about 1.8% and shallow cumulus case by 2.4%. There is increase in hydrolapse by 6% in both cases mainly as a consequence of constant relative humidity and Clausius-Clayperon relationship.

The procedure for derivation of large-scale forcing for the perturbed climate is same as control. At the surface, the horizontal winds remain unchanged from the control, along with a constant relative humidity leads to a reduction in horizontal advection tendency of the specific humidity (Figure 2.1). The assumptions for the perturbed climate lead to a decrease in vertical velocity at Stratocumulus and Shallow Cumulus locations(Figure 2.1) by about 6%. This decrease in  $\omega$  is more due to a change in lapse rate of temperature than the increased radiative cooling.

During the simulations, a relaxation to the initial profiles of temperature and moisture is used above 400 hPa, the relaxation timescale decreases linearly from 24 hours at 400hPa to 3 hours at 100hPa.

## 2.2 EXPERIMENTAL FRAMEWORK

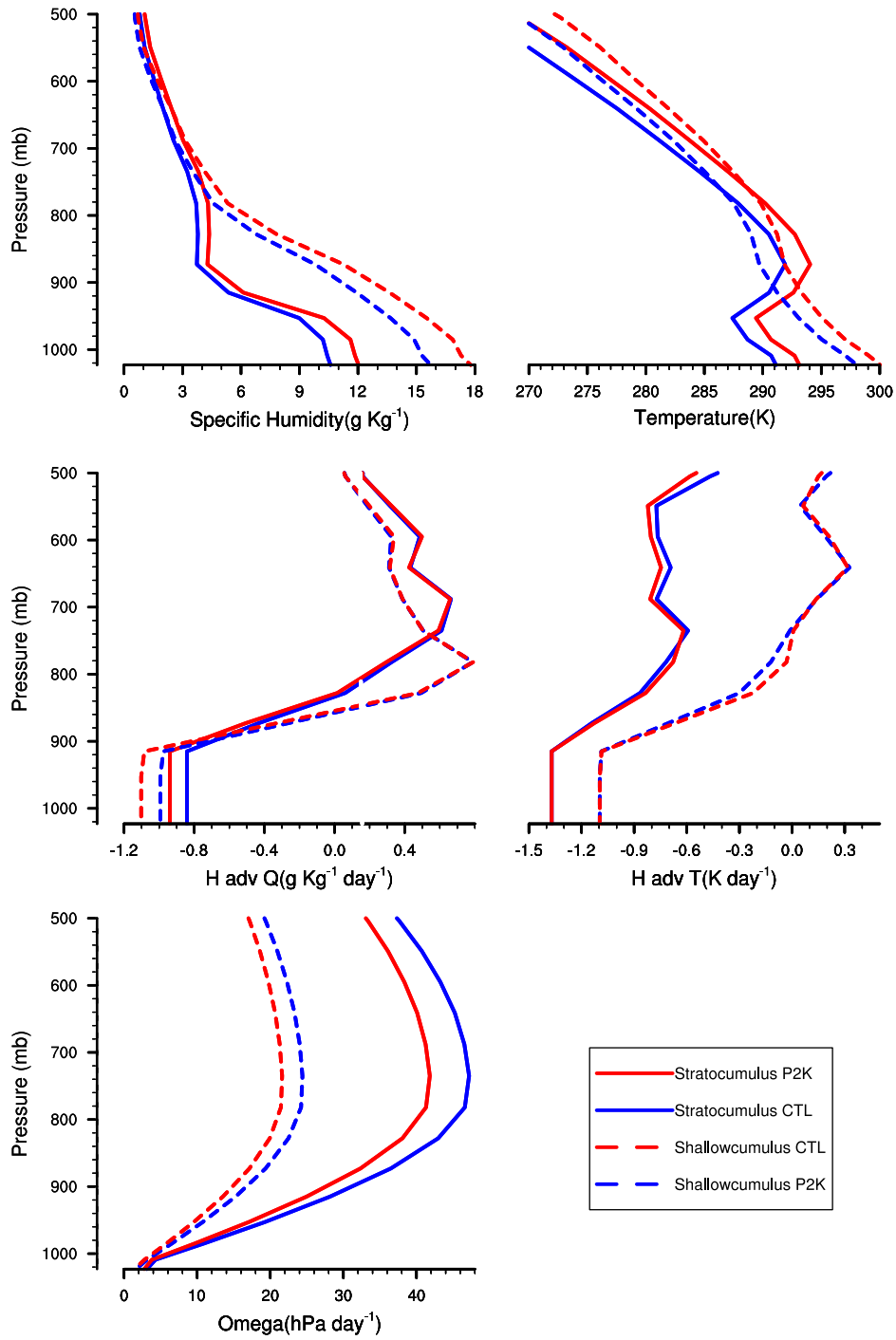


Figure 2.1: Initial conditions and large-scale forcing used for the, Stratocumulus (continuous) and Shallow Cumulus (dashed) cases, and for the control (blue) and the perturbed (red) climate.

### 2.3 Single column model under constant large scale forcing

The Stratocumulus control case under a constant large scale forcing, adjusts to an equilibrium state on order of a month (Figure 2.2(a)). The clouds here are much closer to the surface than expected for the situation, nevertheless the liquid water path is reasonable.

In contrast, the Shallow Cumulus control case under a constant large-scale forcing, transits between two equilibrium states after more than 3 years of simulation (Figure 2.2(b)). The changes in the equilibrium states are marked by a increase in height of cloud layer by one model level and a decrease in mean and variability of liquid water path. The clouds cover here is stronger (100%) and farther (3-4 km) from the surface than expected for the situation, but again the liquid water path is reasonable.

A key aspect here is, if the model was run for less than 3 years, which was typical in the CGILS intercomparison, the solution produced in the Shallow Cumulus case is not representative of the equilibrium. Moreover, there is no feature of the large-scale forcing which induces a 3 year timescale. The parametrizations, as a matter of definition use a statistical equilibrium (eg, quasi equilibrium hypothesis for convection) assumption, they produce a single equilibrium solution under a given largescale forcing. The interactive surface fluxes and radiation here, make the large scale forcing interactive with the solution. Even in such a situation, presense of timescales over 3 years is unreasonable.

To see if more equilibria are generated on longer timescales and the representativeness of the reference equilibrium, we perform a 10 x 10 year ensembles for the Stratocumulus case and a 10 x 50 year ensembles for the Shallow Cumulus case by perturbing the intial conditions. The perturbations were introduced in below 950 hPa in Stratocumulus case and below 800 hPa in the Shallow Cumulus case. The temperature was perturbed by 0.2K and the specific humidity was perturbed by 30%.

All the ensemble simulations of the Stratocumulus case under a constant large-scale forcing reach to a same equilibrium state ( Figure 2.3(a)). Meaning, the reference simulation of the stratocumulus case is well representative.

In contrast the ensembles of the Shallow Cumulus case reach to three different states and the transition can be spontaneous even after 15 years. The unstable state charectrised by a higher variability in liquid water path, transits after certain years to one of the two stable states. After 20 years, aproximately half of the ensembles are in each stable state (Figure 2.4). The mismatch between the pdfs of the ensemble and reference simulation, indicates that the reference simulation

## 2.3 SINGLE COLUMN MODEL UNDER CONSTANT LARGE SCALE FORCING

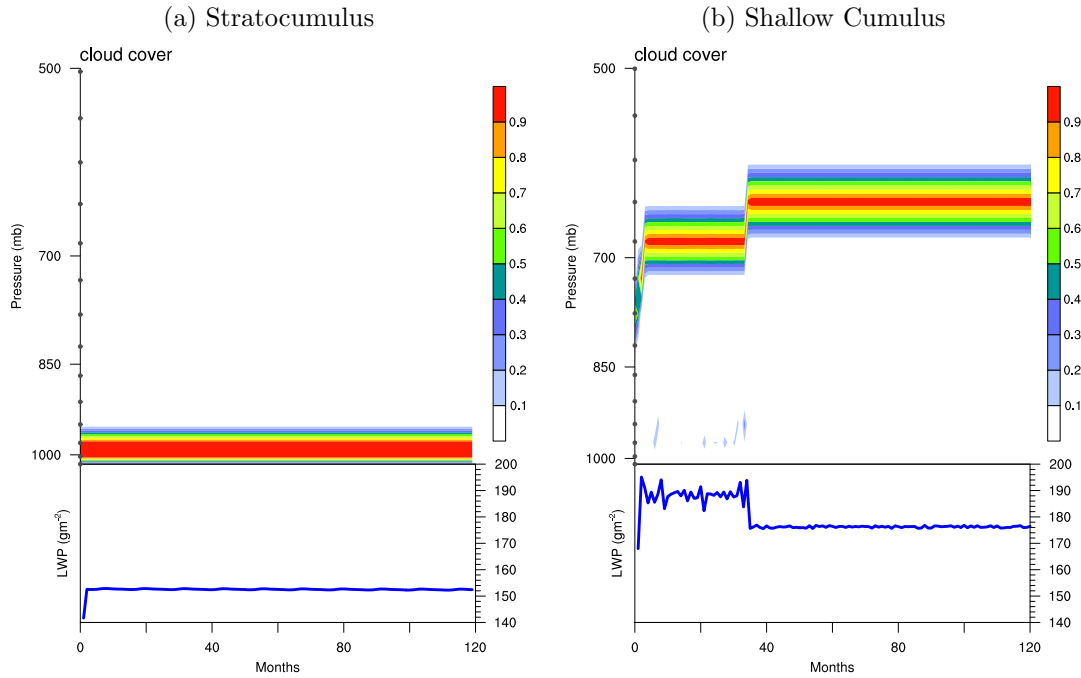


Figure 2.2: Time series (monthly) of simulated cloud cover and liquid water path for the, a) Stratocumulus and b) Shallow Cumulus cases, under a constant large-scale forcing. The grey dots on the vertical axis represent the model vertical grid levels.

of the Shallow Cumulus case is not well representative.

To understand consequences on the CGILS intercomparison, we perform similar experiments with the CGILS perturbed climate and compare the cloud feedbacks. Although the cloud radiative effect (CRE) does not necessarily represent cloud feedback (Soden et al. 2004), here it is still used as a metric for the cloud feedback as we do not expect to have much cloud masking effects over these oceanic locations.

## 2. RESPONSE OF A SINGLE COLUMN MODEL TO A STATIONARY LARGE SCALE FORCING

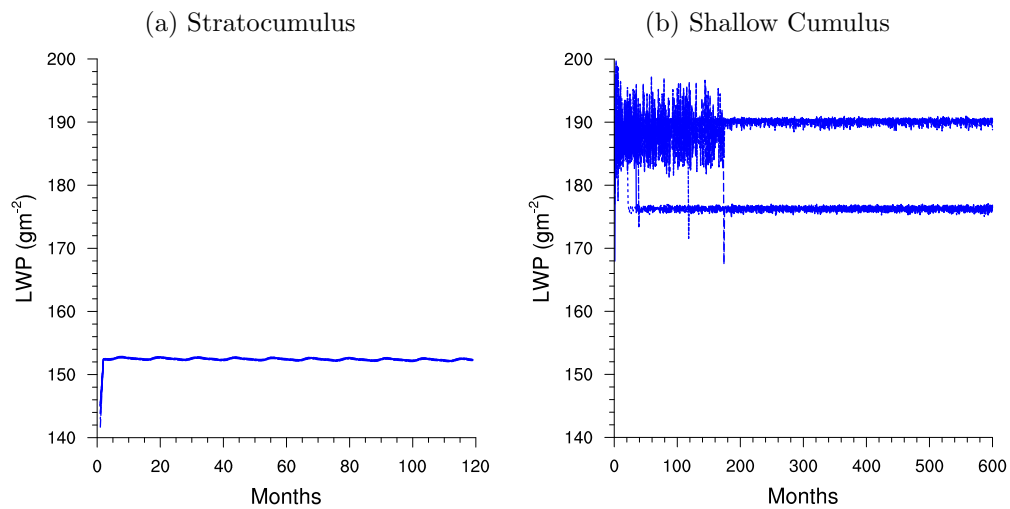


Figure 2.3: Ensemble time series of liquid water path (monthly) for the, a) Stratocumulus and b) Shallow Cumulus cases, under a constant large-scale forcing.

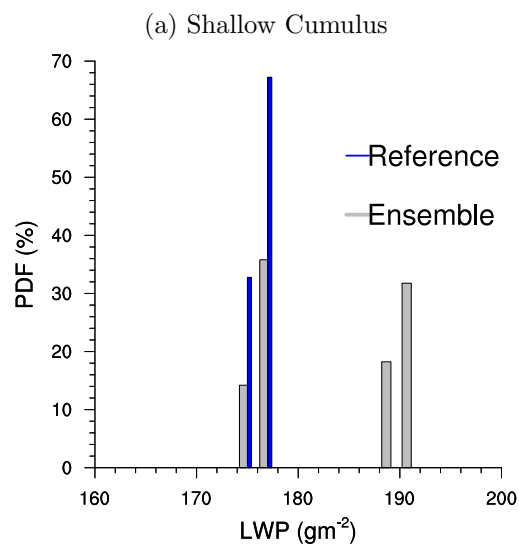


Figure 2.4: Probability Density Function of liquid water path for Shallow Cumulus case under a constant large-scale forcing. The PDFs from the ensemble runs are shown in Black and for the reference simulation in Blue.

### 2.3.1 Idealized low cloud-climate change under a constant large-scale forcing

The Stratocumulus case, subject to an idealistic climate change produces a positive cloud feedback (Figure 2.5(a)). This change in cloud radiative effect indicates that for the imposed idealistic climate change (p2k) clouds cool less efficiently than the control climate (ctrl). The annual cycle in the cloud radiative effect is due to the ozone climatology employed. The positive feedback is more clear in the pdfs of cloud radiative effect (Figure 2.6(a)) and the net change in cloud radiative forcing is about  $+2Wm^{-2}$ .

The Shallow Cumulus case, subject to an idealistic climate change (p2k) produces an ambiguous feedback depending on the member of ensemble. The multiple equilibria in the Shallow Cumulus control case are not visible in the perturbed climate after 10 years. This is more evident in the bi-modal pdf of cloud radiative effect in the control climate, compared to uni-modal pdf of the perturbed climate (Figure 2.6(b)). The net change in cloud radiative effect, by integrating the pdfs is positive and about  $+0.4Wm^{-2}$ .

The absence of large-scale feedback in the single column model does lead to locked equilibrium states in certain situations. To see if the transience in large-scale forcing can mimic the large-scale feedback, we perform experiments with a random, stationary large scale forcing. To get an estimate of variation in the large-scale forcing we look at the ECMWF reanalysis.

## 2.4 Single column model under a stationary, random large scale forcing

ECMWF reanalysis shows a high variability in  $\omega$  sampled at a similar location (Table 2.1) as the Shallow Cumulus case (Figure 2.7). The standard deviation in the vertical velocity is at times more than 100% of the mean. Sometimes, a much higher variance in largescale forcing exists in current climate models, discussed in the Appendix. A random noise with 50% of mean  $\omega$  and vertically coherent is a reasonable starting point. The selected random forcing is introduced every 6 hours.

The cloud cover in both Stratocumulus and Shallow cumulus control cases does not change much under the chosen random large scale forcing (50% mean and introduced 6 hourly) as compared to constant forcing cases (Figure 2.8 and Figure 2.2). This is in contrast with the Brient et al. (2012). The variability in the liquid water path is much more than found in the constant forcing cases, although the mean remains approximately the same. The transition in two equilibrium states

## 2. RESPONSE OF A SINGLE COLUMN MODEL TO A STATIONARY LARGE SCALE FORCING

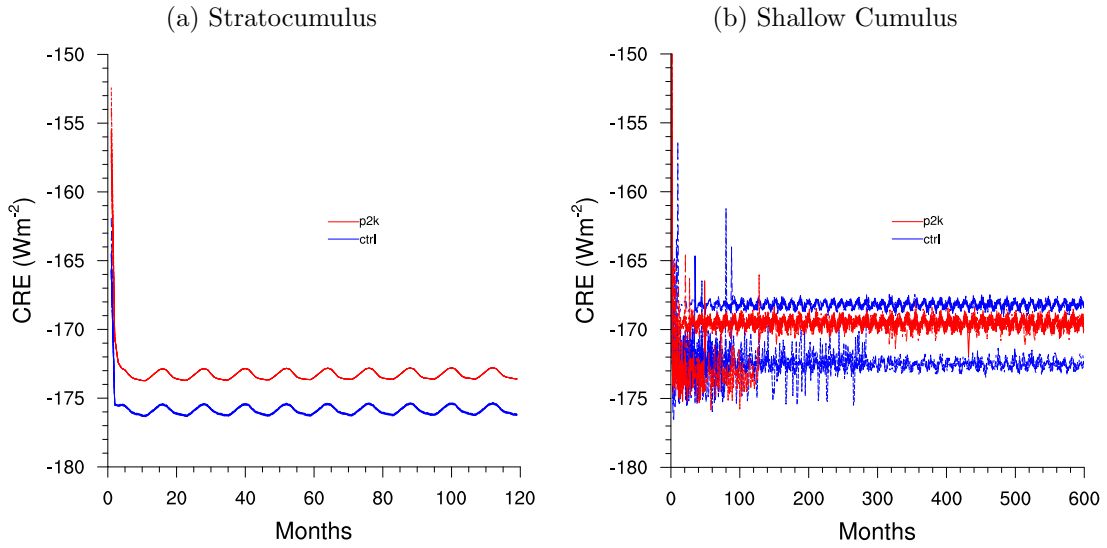


Figure 2.5: Ensemble time series of Cloud Radiative Effect(monthly) for the, a) Stratocumulus and b) Shallow Cumulus cases, under a constant large-scale forcing. The control case is shown in Blue and the perturbed climate in Red.

in the Shallow Cumulus case (Figure 2.8(b)) happens earlier than the case with constant forcing.

To see if the equilibrium solution of the single column model under a random, stationary large scale forcing is representative, we perform 10 ensembles with perturbations in the initial conditions, similar to the Section 2.3.

All the ensemble simulations of the Stratocumulus case under the chosen random large-scale forcing (50% mean and introduced 6 hourly) reach to a same equilibrium (Figure 2.9 (a)). This behavior is similar to that of Stratocumulus case under a constant large scale forcing.

All the ensembles of Shallow Cumulus case under the chosen random large-scale forcing (50% mean and introduced 6 hourly) reach to a same equilibrium (Figure 2.9 (b)). This is more evident in Figure 2.10(a), there is no mismatch in the pdfs of LWP from the ensemble and reference simulations. This behavior is in contrast with the constant large-scale forcing case where model reaches to two different equilibrium solutions. In effect, the random large-scale forcing helps the model to reach a more stable equilibrium, thus making the reference solution under a random, stationary large-scale forcing, representative.

The magnitude and frequency of randomness were somewhat an arbitrary choice, on reducing the magnitude of randomness, the Shallow Cumulus case produces multiple equilibrium states. This is evident in (Figure 2.10(b)), where the pdf of LWP from the ensemble do not match the reference simulation.



## 2.4 SINGLE COLUMN MODEL UNDER A STATIONARY, RANDOM LARGE SCALE FORCING

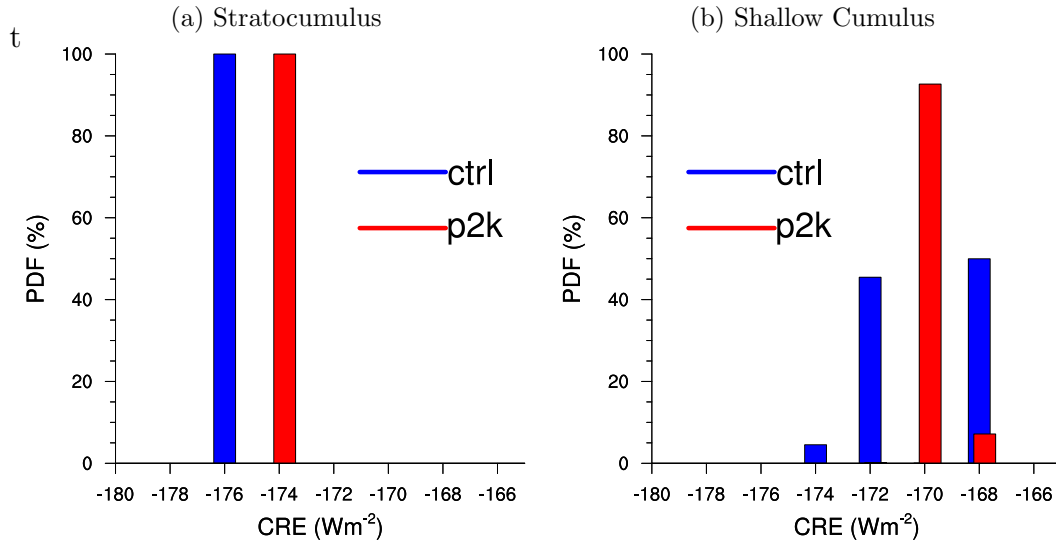


Figure 2.6: Probability Density Functions (%) of Cloud Radiative Effect for the, a) Stratocumulus and b) Shallow Cumulus cases, under a constant large-scale forcing. The control case is shown in Blue and the perturbed climate case in Red. Bin width is  $2 Wm^{-2}$  and the initial months are excluded from the computation.

To see the influence of random, stationary large-scale forcing on the cloud feedbacks, we perform similar experiments with the CGILS perturbed climate and compare the cloud feedbacks.

### 2.4.1 Idealized low cloud-climate change under random large-scale forcing

The Stratocumulus case under the chosen random large-scale forcing (50% mean and introduced 6 hourly) and subject to an idealized climate change (p2k) produces a positive feedback. The positive feedback is clearer from the pdfs of cloud radiative effect (Figure 2.12(a)) and the net change is about  $+2.4 Wm^{-2}$ . This positive feedback is approximately same as the constant forcing case although the variability is higher.

The Shallow cumulus case under the chosen random large-scale forcing and subject to an idealized climate change (p2k) produces a negative feedback. This is more clearly evident from the pdfs of cloud radiative effect in Figure 2.12(b), the net change in cloud radiative forcing is about  $-2.2 Wm^{-2}$ . This negative feedback produced under the random large-scale forcing is in contrast with the net positive feedback produced in constant large-scale forcing case.

To further see the influence of nature of large-scale forcing on the simulated

## 2. RESPONSE OF A SINGLE COLUMN MODEL TO A STATIONARY LARGE SCALE FORCING

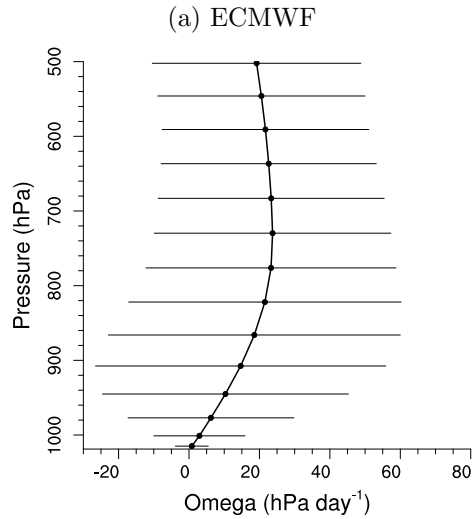


Figure 2.7: Vertical velocity and its standard deviation from the ECMWF reanalysis sampled at a shallow cumulus location in East Pacific, in July 2000.

cloud feedbacks, we perform a 1000 simulations with varying frequency of forcing and the magnitude of forcing. For each square in the Figure 2.13, pdfs from the 10 ensembles for the control and the perturbed climate are integrated to produce the indicated magnitude of CRE.

Broadly, the cloud feedbacks in the model under a random large scale forcing can be grouped into three regions (Figure 2.13): a region where the sign of feedback is clear (positive feedback is indicated by red and negative is indicated by blue), region where feedback is difficult to determine due to multiple equilibria (indicated by hatched region) and region where the variability is high and the pdfs of cloud radiative forcing are statistically difficult to distinguish from each other (indicated by pink).

Overall, the Stratocumulus case produces a positive cloud feedback and the Shallow Cumulus case produces a negative cloud feedback for the stable solutions. The regions of stable solutions are different for both the cases. The stable solutions in Stratocumulus are in lower left of Figure 2.13(a) (at a lower magnitude and higher frequency of large-scale forcing) and the stable solutions for Shallow Cumulus are in middle of 2.13(b) (moderately forced situations). Under a very strong forcing (upper right part of the Figure 2.13), the feedbacks are statistically difficult to distinguish in both the cases. A positive cloud feedback in the Stratocumulus case and a negative cloud feedback in Shallow cumulus is robust.

## 2.4 SINGLE COLUMN MODEL UNDER A STATIONARY, RANDOM LARGE SCALE FORCING

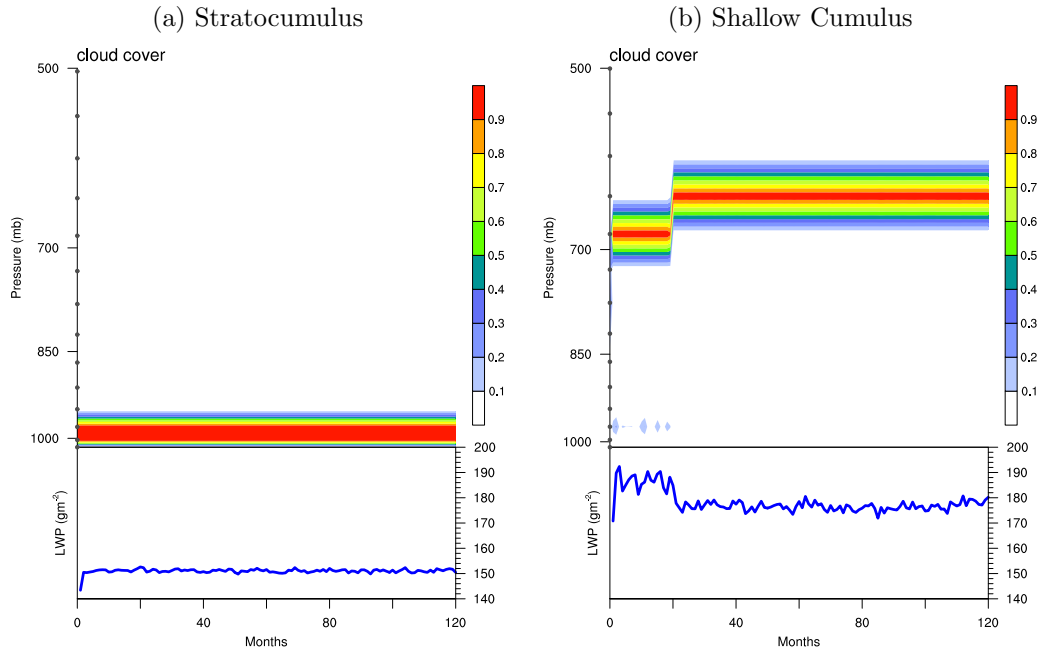


Figure 2.8: Time series (monthly) of simulated cloud cover and liquid water path for the, a) Stratocumulus b) Shallow Cumulus cases under a random large scale forcing. The random forcing applied is 50% of mean vertical velocity and introduced every 6 hours. The Grey dots on the vertical axis indicate the model vertical grid levels.

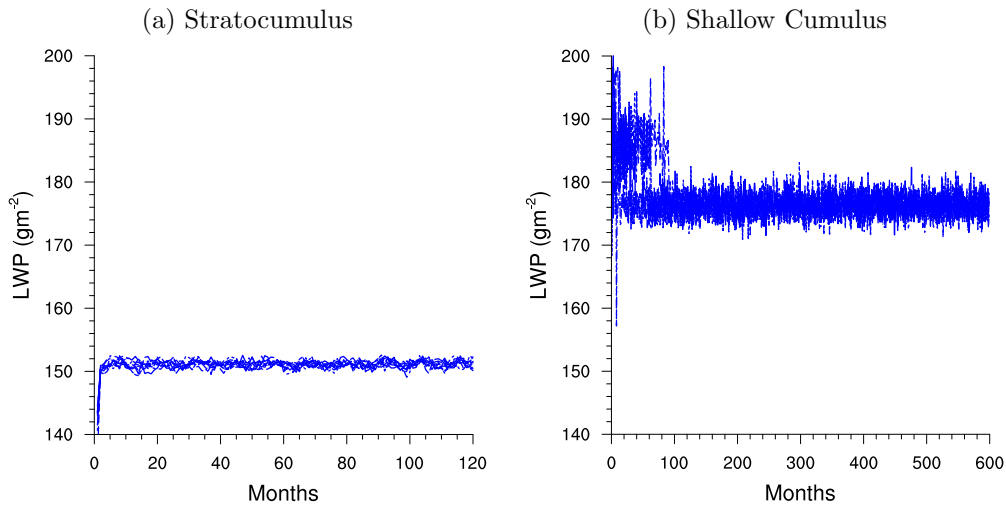


Figure 2.9: Ensemble time series of liquid water path(monthly) for the, a) Stratocumulus b) Shallow Cumulus cases, under a random large-scale forcing. The magnitude of large scale forcing applied is 50% of the mean vertical velocity and introduced every 6 hours.

## 2. RESPONSE OF A SINGLE COLUMN MODEL TO A STATIONARY LARGE SCALE FORCING

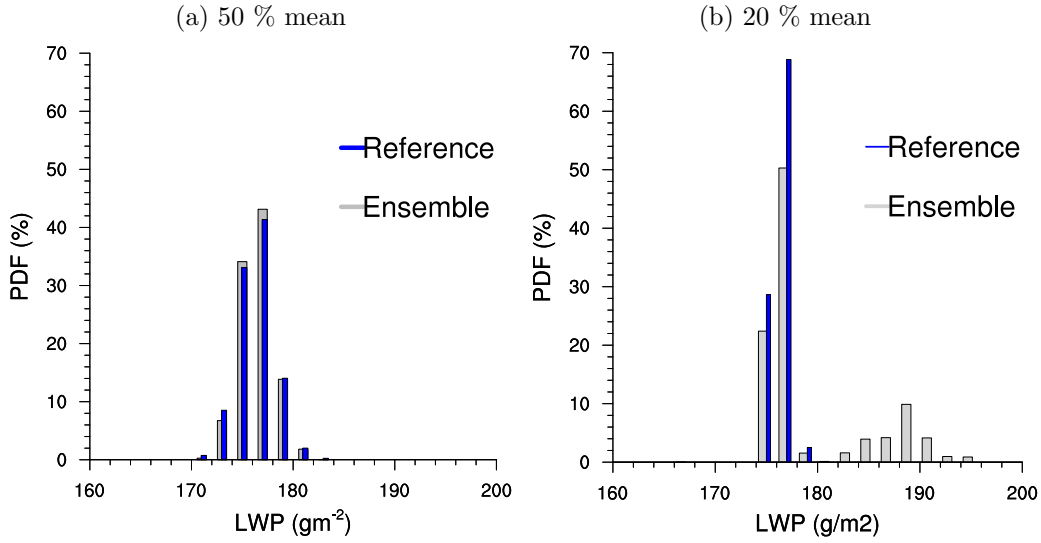


Figure 2.10: Probability Density Function (%) of liquid water path for the Shallow Cumulus cases under random large-scale forcing, with magnitude a) 50 % of mean, introduced every 6 hours and b) 20 % of mean, introduced every 6 hours. The PDFs from the ensemble runs are shown in Grey and for the reference simulation in Blue.

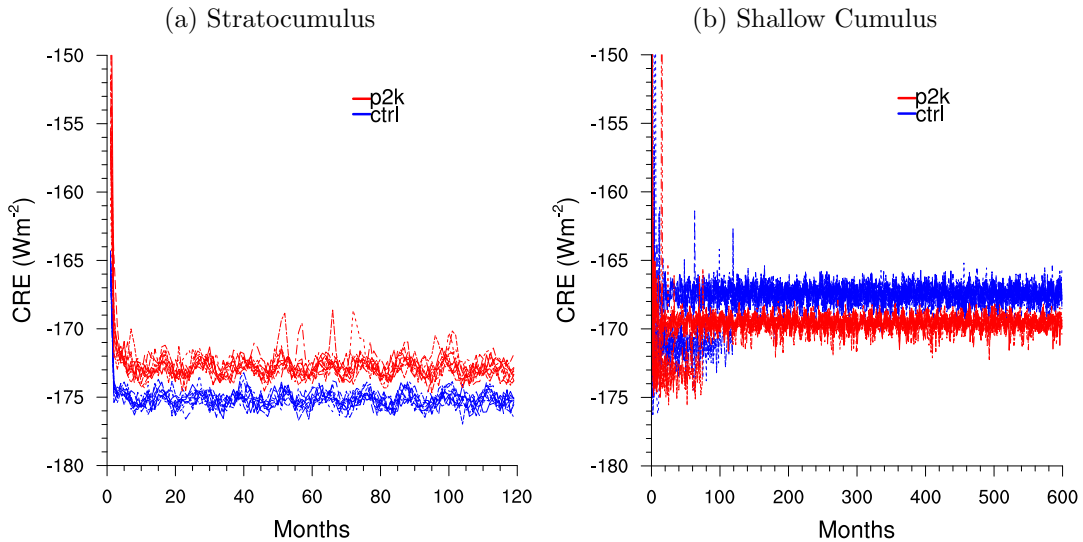


Figure 2.11: Ensemble time series of Cloud Radiative Effect(monthly) for the, a) Stratocumulus and b) Shallow Cumulus cases, under a random large-scale forcing. The control climate is shown in Blue and the perturbed climate case in Red. The magnitude of large scale forcing applied is 50% of the mean vertical velocity and introduced every 6 hours.

## 2.4 SINGLE COLUMN MODEL UNDER A STATIONARY, RANDOM LARGE SCALE FORCING

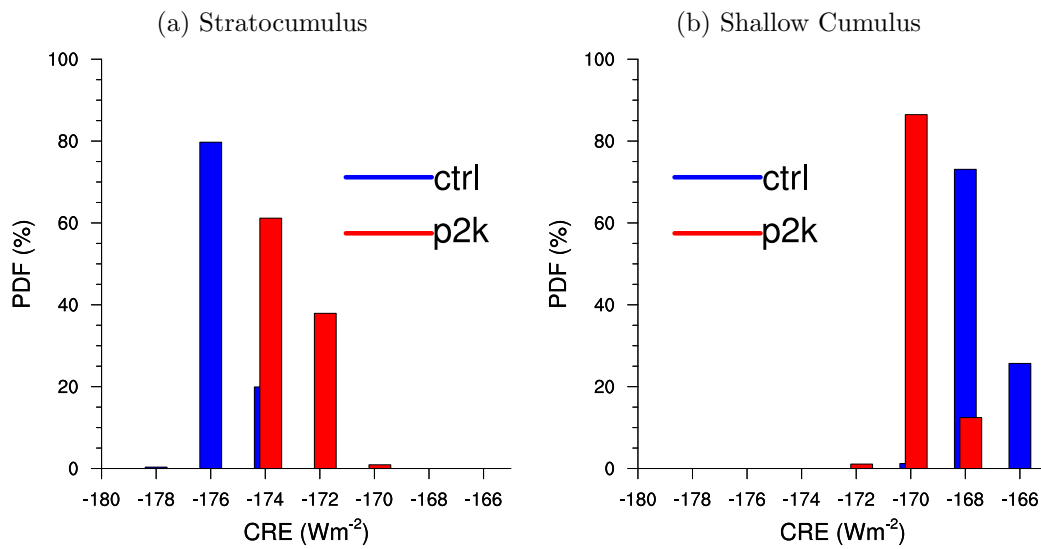


Figure 2.12: Probability Density Functions (%) of Cloud Radiative Effect for the, a) Stratocumulus and b) Shallow Cumulus cases under a random large-scale forcing. The control climate is shown in Blue and the perturbed climate case in Red. The magnitude of large scale forcing applied is 50% of the mean vertical velocity and introduced every 6 hours. Bin width is  $2 Wm^{-2}$  and the initial months are excluded from the computation.

## 2. RESPONSE OF A SINGLE COLUMN MODEL TO A STATIONARY LARGE SCALE FORCING

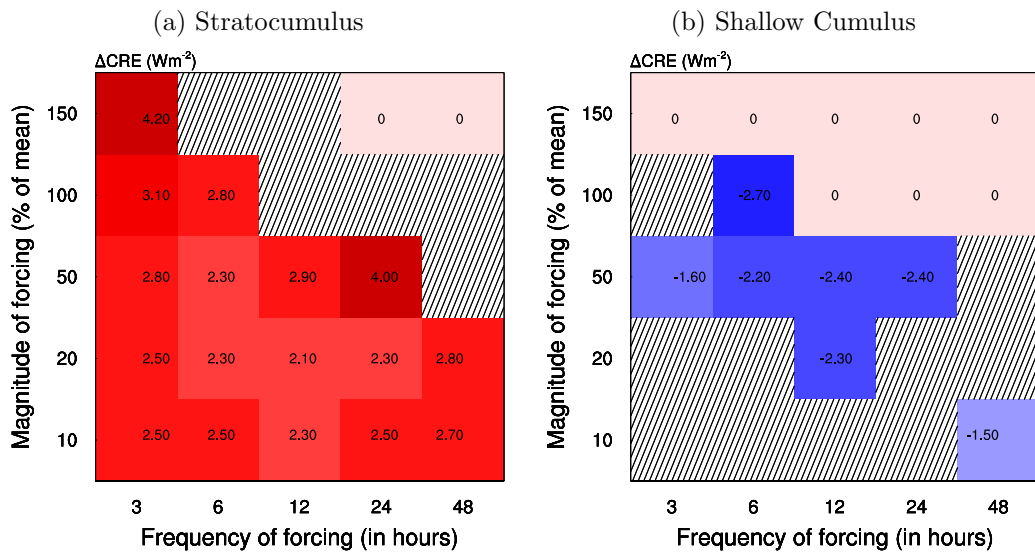


Figure 2.13: Change in Cloud Radiative Effect ( $Wm^{-2}$ ) for the, a) Stratocumulus and b) Shallow Cumulus cases under a random large-scale forcing of varying magnitude but same mean. The vertical axis represents the magnitude of large scale forcing applied, (% of the mean vertical velocity) and the horizontal axis represents frequency over which the forcing is used. Hatched regions are the locations where the change in Cloud Radiative Effect is uncertain.

## 2.5 Conclusions and Outlook

In summary we studied the equilibrium response of ECHAM6 single column model to the nature of large-scale forcing used. The model sensitivities can underscore the potential advantages of a single column model study using an idealized forcing, such as CGILS. Under a constant large-scale forcing the equilibrium solutions of a single column model are not necessarily well representative. A time varying large-scale forcing, mimicing the large scale feedback was important for making the solutions representative. A random, stationary forcing with 50% of mean and introduced 6 hourly was reasonable for ECHAM6. In contrast to (Brient and Bony 2012), the mean solution in ECHAM6 did not change under a random large scale forcing, the forcing mainly helped the model to reach a stable state. ECHAM6 subject to idealized CGILS climate change, produces a robust positive feedback at Stratocumulus and robust negative feedback at the Shallow Cumulus locations.

It is important to understand the reasons for any such behavior of the single column model. Given that the transitions in the equilibrium states under constant forcing are accompanied by changes in one model level, it is important to investigate the role of numerical representation in the cloud feedbacks. Sensitivity of model to temporal and vertical resolution and possible reasons for such a behavior of single column model are part of another study not included in the thesis.

To be able to translate any results from the CGILS intercomparison to a full complex, coupled model, it is necessary to investigate the representativeness of CGILS climate change to that of a full complex, coupled model over similar locations. These questions form topics for the subsequent chapters.





# Chapter 3

## Low-cloud feedbacks in ECHAM6 and CGILS forcing

### 3.1 Introduction

Understanding response of low-clouds to a changing climate in a comprehensive climate model remains a complex task. Treating this complexity often mandates a use of hierarchy of simplified model configurations subject to a surrogate climate change. For instance, an uncoupled atmosphere model prescribed with observed SST is often used as an analog for studying responses in a coupled model. A further simplification of this analog is an aquaplanet, where the entire surface is replaced by an ocean and zonally symmetric SSTs are prescribed. More recently, Zhang and Bretherton (2008); Zhang et al. (2012) proposed idealized climate change experiments using a single column model to understand physical mechanisms of low cloud feedbacks. This was later turned into an intercomparison of different single column models (CGILS intercomparison) in an aim to understand differences in low-cloud feedbacks among their comprehensive configurations.

Every simplified configuration in such hierarchy is often a compromise of a large scale feature. For example, in an uncoupled AMIP configuration, a frequently used surrogate climate change is a uniform increase in SST. A uniform increase in SST treats clouds as a response to surface temperature and not vice versa, in addition it does not represent changes in surface temperature gradients of the coupled configuration, which can lead to changes in convergence/divergence. These missing features can be argued to contribute to differences in their low-cloud feedbacks.

A single column model needs a large scale forcing along with the SST at the boundary. Thus for a surrogate climate change using a single column model would mean designing changes in large scale forcing in addition to increase in surface temperature. Designing such idealized climate change which is representative of large scale changes in their GCMs is a challenging task. The response of single

### 3. LOW-CLOUD FEEDBACKS IN ECHAM6 AND CGILS FORCING

column model may not be indicative of the response of more comprehensive model if the essential changes in forcings are not captured by the surrogate climate change. This motivates us to consider the question how do low clouds differ in the frequently used hierarchy of simplified configurations using MPI-ESM-LR? The single column model experiments performed for CGILS intercomparison and output from CMIP5 provide an opportunity to study some of these aspects.

In this chapter, we study cloud feedbacks in the hierarchy of MPI-ESM-LR, GCM configurations at shallow cumulus and stratocumulus locations defined by using CGILS largescale state. The remainder of the Chapter is organized as follows, selection of relevant sets of experiments in CMIP5 and overview of cloud feedbacks in these sets is described in Section 3.2. Strategy to compare the MPI-ESM-LR single column to other GCM configurations is discussed in Section 3.3. Response of clouds in CGILS and similar locations in the hierarchy of GCM configurations is presented in Section 3.4. The changes in large scale environment at these locations are presented in Section 3.5. Conclusions and Outlook are presented in Section 3.6.

## 3.2 Overview of relevant CMIP5 experiments

There are about 108 experiments conducted under CMIP5 (Taylor et al. 2012), however not all the experiments were performed by MPI-ESM-LR. Of interest is an experiment set representative of changing climate across a hierarchy of GCM configurations: atmosphere-ocean coupled configuration, uncoupled atmosphere GCM configuration, and aquaplanet configuration.

For the coupled configuration, equilibrium experiment with greenhouse gasses fixed at pre-industrial level serves as a reference control experiment (piControl). This piControl subject to an abrupt increase in CO<sub>2</sub> by 4 times (abrupt4xCO<sub>2</sub>) serves as a perturbed climate experiment. Among the various coupled configuration experiments performed for CMIP5, piControl is selected as a reference, mainly because it is an equilibrium experiment as opposed to historical experiments with changing aerosols, greenhouse gasses and land use changes. Monthly output diagnostics from last 20 years of piControl are used for the analysis.

For the atmosphere-only configuration, the experiment with prescribed observed monthly SST over the oceans serves as a control experiment (amip) and the experiment with SST of amip increased by 4K serves as a perturbed climate experiment (amip4K). Due to cheaper computational cost, this configuration is frequently used as an analog for the coupled model and it is the most preferred configuration during development of an atmospheric model. Monthly output diagnostics for the years 1988-2008 are used for the present analysis.

### 3.2 OVERVIEW OF RELEVANT CMIP5 EXPERIMENTS

<b>Experiments</b>	<b>Time</b>	<b><math>\Delta</math>SST(K)</b>	<b><math>\Delta</math>CRE(<math>Wm^{-2}</math>)</b>
abrupt4xCO2 - piControl	—20 years	4.6	2.87
amip4K - amip	1988-2008	4.0	2.76
aqua4K - aquaControl	years 3-5	4.0	-4.11

Table 3.1: Overview of MPI-ESM-LR CMIP5 experiments: Number of years considered, change in SST and CRE over tropical (40S to 40N) oceans

For the aquaplanet configuration, an experiment with a zonally symmetric SST, idealized from observed climatology (Qobs from Neale and Hoskins (2000)) serves as a control experiment (aquaControl) and the experiment with SST of aquaControl increased by 4K serves as a perturbed climate experiment. This configuration is frequently used to understand aspects of the tropical largescale atmospheric circulations, increasingly it has been used to study the role of tropical clouds in large scale circulations. Using two aquaplanets Medeiros et al. (2008) showed that they capture the climate sensitivity of the AMIP configurations. Monthly output diagnostics from the third year of the aquaplanet simulations are used for the present analysis.

We use change in cloud radiative effect as a metric for the cloud feedback. CRE is defined as the difference in net top of atmosphere downward radiation with and without clouds. A positive CRE would mean that the greenhouse effect dominates the cooling due to reflection of shortwave radiation. For the tropical marine boundary layer clouds, considered in this study, CRE is negative. Their proximity to surface ensures that they do not alter the effective emissivity of the atmosphere, whereas their albedo contributes to the cooling effect of the planet. A change in this CRE ( $\Delta$ CRE) among two experiments reflects a change in cloud properties to cool/warm the planet. Although this  $\Delta$ CRE is not necessarily indicative of a cloud feedback due to cloud masking effects (Soden et al. 2004), given the interest is over tropical oceanic locations where masking effects are stationary this is not an issue. For instance Vial et al. (2013) showed that the changes in CRE and cloud feedbacks from other methods are well correlated over tropical oceans. Besides, the simplicity in defining the metric is rather an advantage.

Table 3.1 shows an overview of MPI-ESM-LR, CMIP5 experiments used in the study. The annual averaged change in sea surface temperature is slightly higher in the coupled model. The overall tropical cloud feedback is positive and similar in coupled and amip configurations. Figure 3.1 shows that the regions that contribute to this tropical cloud feedback are also similar in both coupled and amip configurations. The negative feedbacks are mainly associated with South-

### 3. LOW-CLOUD FEEDBACKS IN ECHAM6 AND CGILS FORCING

ern ITCZ in Pacific and Atlantic, however these changes are much stronger in the coupled model. The positive feedbacks are associated with Northern Pacific and Atlantic regions, the changes are stronger at the subtropical low-cloud regions. The similarity in cloud feedbacks of amip and coupled configurations is remarkable, given the differences in the configurations. The cloud feedback in the aquaplanet is negative. There is a strong negative feedback in the deep convective regime, outside this regime, there are alternating latitudinal bands of weaker positive and negative feedbacks, but the total area of regions with negative feedback being much larger, leads to a net negative feedback. This different response of aquaplanet compared to amip or coupled model is slightly surprising because, using a previous version of MPI-ESM-LR, Medeiros and Stevens (2011) showed that it captured the core distribution of large scale features of an atmospheric GCM. Nevertheless, it is still possible for the sensitivity of the aquaplanet to be different than the amip configuration.

### 3.2 OVERVIEW OF RELEVANT CMIP5 EXPERIMENTS

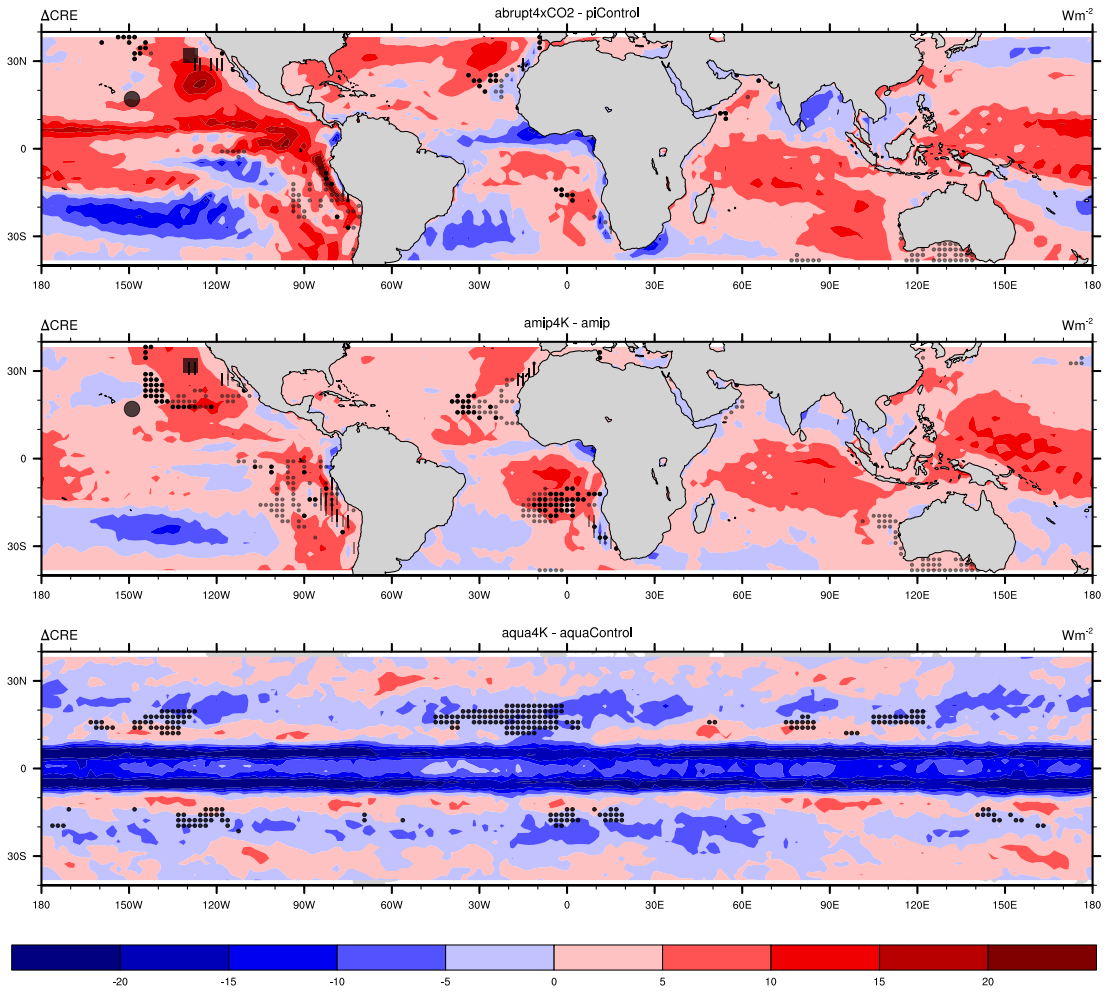


Figure 3.1: Annually averaged change in Cloud Radiative Effect ( $Wm^{-2}$ ) for the selected CMIP5 experiment sets. CGILS, Stratocumulus and Shallow Cumulus locations are indicated by a circle and square. CGILS-like Stratocumulus and Shallow Cumulus locations are indicated by lines and dots. Summer-like points are indicated by darker dots and lines.

### 3.3 Sorting CGILS and CGILS-like locations

A direct way to compare the CGILS idealized single column model experiments to the GCM configurations is to pick relevant CGILS geographical locations ( Table 3.2, S6 and S11 locations ) in GCMs and compare the cloud feedbacks. However, the large scale conditions at these CGILS locations in the GCMs can be different than the large scale conditions in the ECMWF reanalysis, on which the CGILS control climate is based. Therefore, it is also desirable to study the responses at locations with large scale conditions in the control experiments similar to that of CGILS control climate (CGILS-like locations). This approach provides a possibility to translate any understanding from localized CGILS locations to larger regions, therefore illustrates the utility of CGILS framework. Besides, the precise geographical location is not possible to translate to an aquaplanet.

This necessity to sort the clouds based on large scale state often arises when studying clouds. Bony et al. (2006) used vertical velocity at 500hPa ( $\Omega$ ) to separate cloud feedbacks as a function of dynamical regime and using this they concluded that most uncertainty in cloud feedbacks in current models arises mainly from the regions of subsidence, the low cloud regions. (Medeiros and Stevens 2011) further sorted the low clouds using lower tropospheric stability (LTS) into shallow cumulus and stratocumulus clouds based on regimes defined by Klein and Hartmann (1993). A similar approach is followed here, every geographical location in the control climate is assigned a regime based on the mean  $\Omega$  and LTS at that location. Locations with LTS and  $\Omega$  similar to the CGILS control climate are marked as “CGILS-like” locations and the changes at these locations in the perturbed climate are examined. Table 3.2 shows largescale conditions for selecting CGILS-like locations. Before we examine the cloud feedback at these locations, we demonstrate the sorting method.

Figure 3.2 shows average cloud top height sorted based on the large scale state in the three CMIP5 experiment sets. The advantage of sorting is rather obvious; sorting clouds using both  $\Omega$  and LTS cleanly separates the clouds into low and high clouds than using just the vertical velocity. The cloud heights in piControl and amip are remarkably similar given, the differences in amip and coupled configurations. The number of types of regimes in aquaControl is small, the regions of strong stability are absent in the aquaControl. Medeiros and Stevens (2011) identified this due to absence of asymmetric cold eastern upwelling regions in the aquaplanet. The frequency of occurrence of each of regimes is indicated by grey contours, the area of subsiding regions is slightly higher in the piControl compared to amip. In Figure 3.2, the CGILS-like Stratocumulus and Shallow cumulus are indicated by a hatched dots and lines. As expected, the average cloud top height for the shallow cumulus like locations (around 900hPa) is higher

### 3.3 SORTING CGILS AND CGILS-LIKE LOCATIONS

Shallow Cumulus		Stratocumulus	
S6	S6 like	S11	S11 like
15.5N<lat<18.5N	15<Omega<25	30.5N<lat<33.5N	35<Omega<45
147W<lon<150W	16<LTS<17	128W<lon<131W	21<LTS<22

Table 3.2: Overview of CGILS and CGILS-like locations

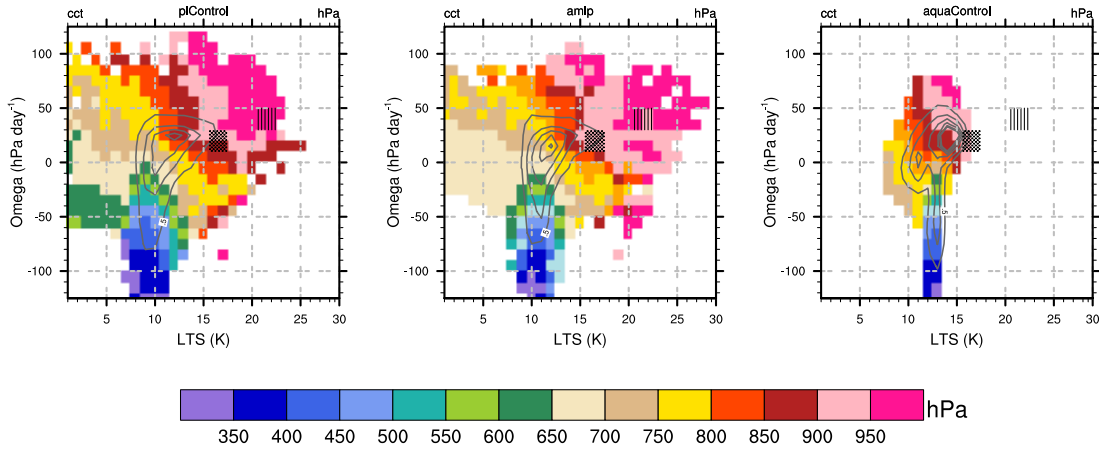


Figure 3.2: Average cloud top height sorted based on omega at 500hPa and LTS. Joint distribution of omega and LTS are showed by black contour lines with 1% intervals. CGILS-like Stratocumulus and Shallow Cumulus locations, are indicated by shaded regions with lines and dots respectively.

than Stratocumulus like locations (around 950hPa) and both of them lie within the expected planetary boundary layer height. GPCI like locations lie at regimes along the line joining Stratocumulus and Shallow Cumulus like locations; increasing cloud height along this transect is reasonably represented in the control experiments.

Figure 3.1 shows the geographical locations corresponding to the CGILS and CGILS-like points. If the geographic points of CGILS are not identified as CGILS-Like then it reflects the differences in the large scale state of control experiments as compared to the re-analysis. Presence of these CGILS-like locations at the eastern boundary current regions (Klein and Hartmann 1993) is indicative of reasonable simulation of large scale in the model. In aqua planets the marginal sampling show up in the plot, the CGILS-like locations are not zonally uniform. As CGILS is based on boreal summer time large scale conditions, in subsequent sections we use only output from boreal summer for coupled and amp configurations.

## 3.4 Response in CGILS and CGILS-like regions

Figure 3.3 shows change in boreal summer CRE sorted on the large scale regimes. The tropical change in CRE is due to positive and negative cloud feedbacks lying in both convecting and subsiding regions. A negative cloud feedback is stronger and predominant in the aquaplanet. There is a positive cloud feedback in Shallow Cumulus like locations in both amip and coupled model and stronger than that at the Statocumulus like locations. GCM configurations have a strong tendency to have compensating shortwave and longwave feedbacks. This tendency is stronger in the coupled configuration. In Single column the difference is mainly due to shortwave changes. It is interesting to understand what causes the differences in the GCMs. These changes at CGILS and CGILS-like locations per degree change in surface temperature are summarized in Figure 3.4.

The differences in shortwave and longwave forcing show that the reasons for the feedback are likely to be different in single column and GCM configurations. The differences in response could be due to different changes in large scale forcing at the CGILS locations. The utility of CGILS lies on the representativeness of idealized climate change to that in a comprehensive GCM at corresponding locations. It is therefore interesting to examine the changes in large scale state in the CGILS-like locations. There by, it also puts to test some of understanding of large scale circulations embedded in deriving CGILS idealized climate change. Before we look at possible location it is useful to summarize the derivation of CGILS largescale forcing.



### 3.4 RESPONSE IN CGILS AND CGILS-LIKE REGIONS

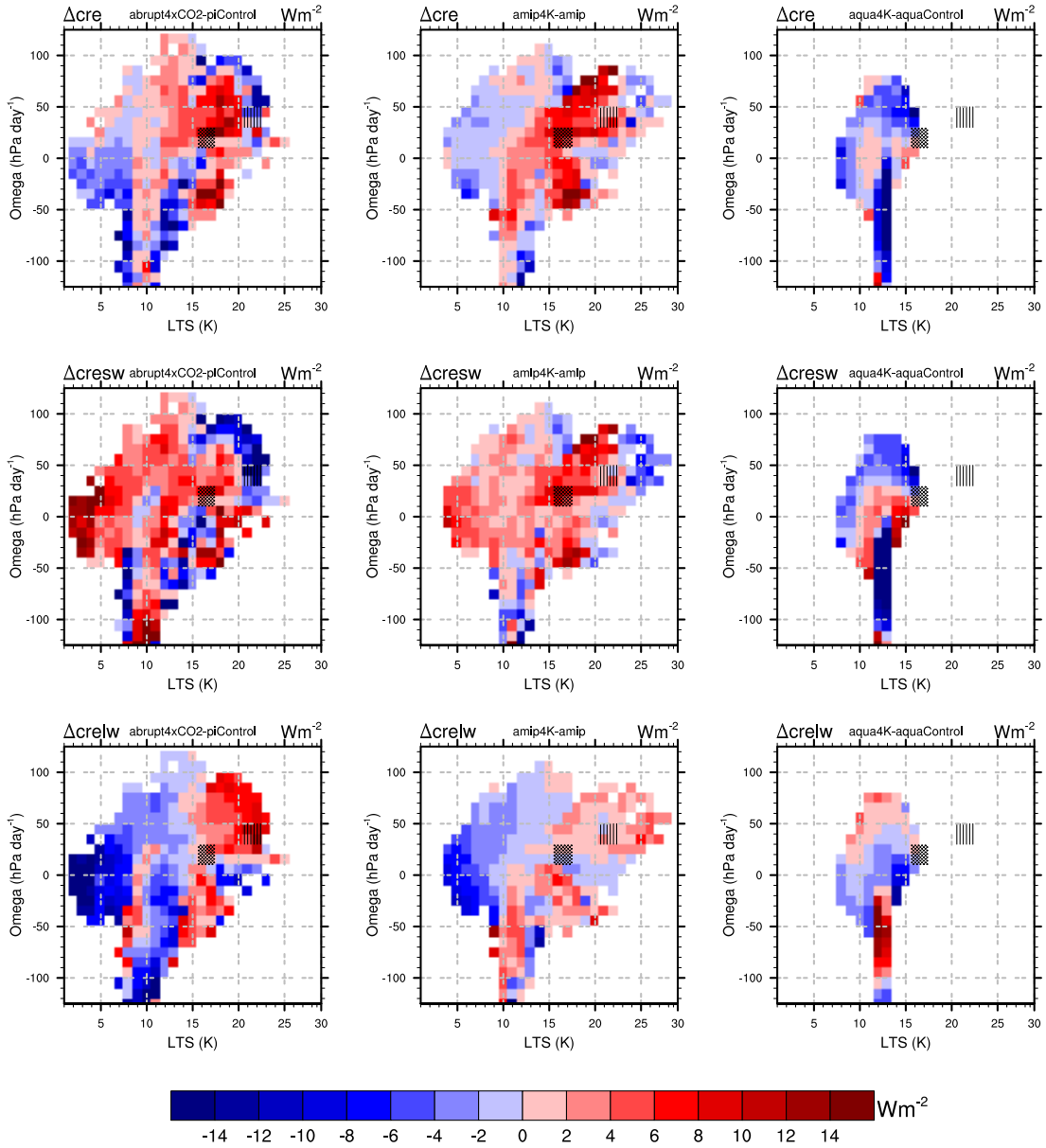


Figure 3.3:  $\Delta$ Cloud Radiative Effect ( $Wm^{-2}K^{-1}$ ) per degree of surface temperature change, during boreal summer in the selected CMIP5 experiments. CGILS-like Stratocumulus and Shallow Cumulus regions are hatched with lines and dots.

### 3. LOW-CLOUD FEEDBACKS IN ECHAM6 AND CGILS FORCING

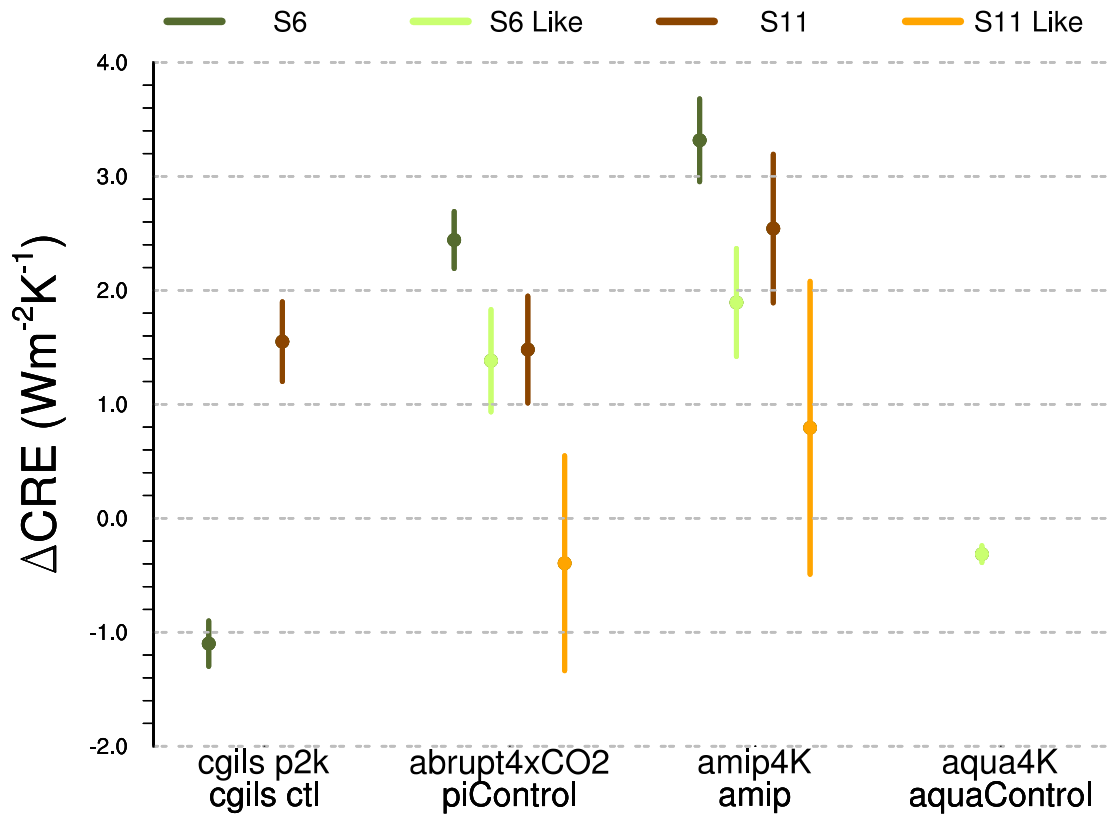


Figure 3.4: Cloud feedbacks ( $Wm^{-2}K^{-1}$ ) at CGILS and CGILS-like locations for the selected heirarchy of configurations.

## 3.5 Forcing and Feedback mechanisms at CGILS Locations

In convecting regions of tropics, with an increase in surface temperature, warmer and moister parcels as they rise condense more vapor; the temperature reduces more slowly with height. These changes in temperature are propagated to large subsiding areas by wave propagation, as the tropical atmosphere cannot sustain the horizontal gradients. Thus a thermodynamic change in temperature profile in tropics can be modeled as changes in moist adiabat over convecting regions. This change in the moist adiabat is fundamental to a thermodynamic climate change such as CGILS. This decrease in temperature lapse rate: with an assumption of constant relative humidity leads to a change in lapse rate of vapor; the radiative cooling increases above the boundary layer and subsidence required to balance this radiative cooling changes.

Lower tropospheric stability, in CGILS increases following the thermodynamic arguments laid above. The increase is 2.3% per Kelvin at S6 and 1.9% per Kelvin at S11. Figure 3.5 shows changes in LTS at the marked locations in the GCMS, there is an overall increase in LTS, but the magnitude differs. The LTS increase in shallow cumulus locations is slightly higher than the stratocumulus locations, this relation is well represented. Klein and Hartmann (1993) showed seasonal variations in cloud cover over stratocumulus cloud regions correlated strongly with LTS. The increase in stability can lead to increase in low cloud cover (eg: Miller (1997)). It can be seen from Figure 3.7 that there is no such correlation with increase in LTS to cloud cover. At S11 like in the coupled model an increase in shortwave can be related to increase in cloud cover. Changes in shortwave are more correlated to changes in liquid water path.

Hydrolapse (HYL) defined as difference in specific humidity at lowest model level and at 700 hPa increases following thermodynamic climate change (Held and Soden (2000), Rieck et al. (2012)). Increase in HYL in CGILS locations is about 5% and similar at CGILS stratocumulus and shallow cumulus locations. There is an increase in HYL in the GCM configurations but the magnitude of increase is much small (Figure 3.5). When other factors remain same, an increase in HYL would mean increase in entrainment of dry air aloft leading to dilution of cloud. There is association between changes in HYL and changes in liquid water path in coupled and amip configurations (Figure 3.7 ). This has potential to explain to why there is stronger decrease in liquid water path in both amip and coupled models at S6-like locations compared to S11-like locations in general. This also could explain why there is decrease in liquid water path at S11-like locations in amip where as there is increase in liquid water path in coupled configuration.

### 3. LOW-CLOUD FEEDBACKS IN ECHAM6 AND CGILS FORCING

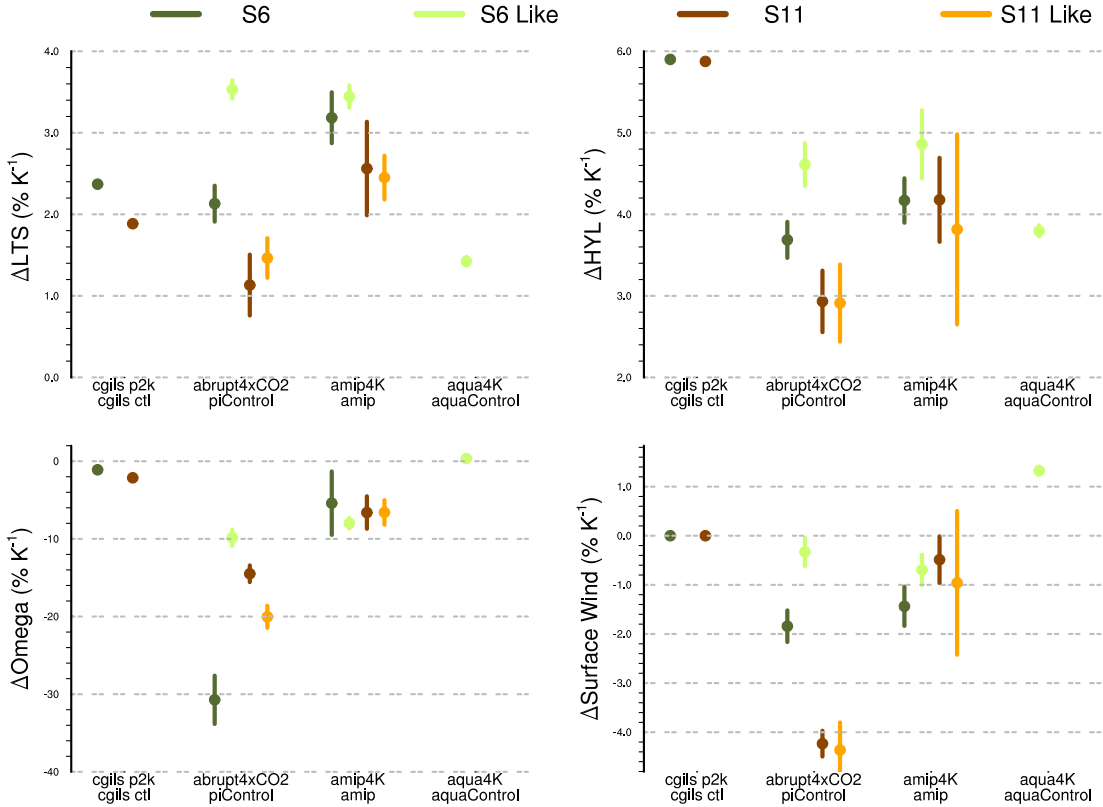


Figure 3.5: Percentage changes in largescale state at CGILS and CGILS-like locations, in the selected hierarchy of model configurations. The values indicated for CGILS single column are based on initial profiles of experimental design.

In the subsiding regions the balance between radiative cooling and subsidence warming is often expected, as in Equation 2.1. This leads to a decrease in vertical velocity corresponding to an increase in adiabatic lapse rate and an increase in vertical velocity corresponding to an increase in clearsky radiative cooling associated with changes in specific humidity and temperature at upper layers. The change in adiabatic lapse rate is more compared to that of increased cooling in the free troposphere, this leads to a decrease in vertical velocity at a rate slightly less than that of LTS. Changes in vertical velocity at CGILS is around 2% at both S6 and S11 locations. The changes in vertical velocity in the hierarchy of configurations are shown in Figure 3.5. Vertical velocity decreases relatively strongly in the GCMs, the changes are much stronger in the coupled model. When other factors remain same a decrease in subsidence should lead to increase in cloud top height, this is one of the mechanisms often argued to lead to positive low cloud feedbacks. In the GCM configurations the decrease in subsidence is not clearly associated with changes in cloud top height (Figure 3.7). It is therefore likely that these changes in clouds at the S6-like and S11-like locations are driven by changes close to the

### 3.5 FORCING AND FEEDBACK MECHANISMS AT CGILS LOCATIONS

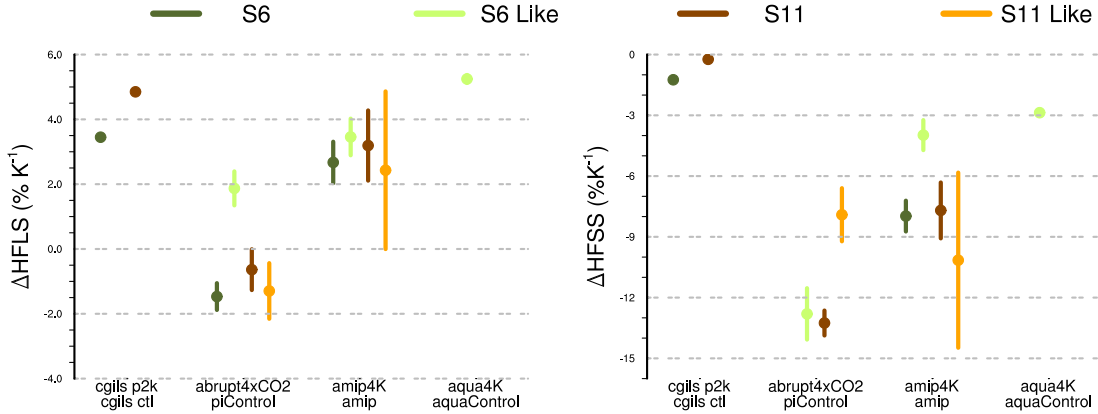


Figure 3.6: Percentage changes in surface fluxes at CGILS and CGILS-like locations, in the selected hierarchy of model configurations. The values indicated for CGILS single column are based on the equilibrium simulations by using single column model.

surface.

Changes in surface winds are assumed to be negligible in CGILS. In the GCM configurations the surface winds decrease (Figure 3.5), consistent with other studies (Richter and Xie 2008). Corresponding to decrease in wind speed sensible heat fluxes decrease more in the GCM configurations (Figure 3.6). The expected increase latent heat flux based on Clausius Clapeyron is 6% at S6 and 6.3% at S11, but the energetic constraints dictate that the changes in latent heat fluxes are often less globally (Held et al. 2006). There can be significant differences regionally. There is increase in latent heat flux at all locations in amip and Single Column Model. Except for s6-like location, the latent heat flux in the coupled configuration decreases in CGILS locations. This is rather surprising, the only reason this can be possible is strong increase relative humidity inside the boundary layer at these locations in the coupled model. Figure 3.9 shows increase in boundary layer relative humidity at s11-like locations in the coupled model is about 30 percent. These changes are possible only because of changes in horizontal advection inside the boundary layer.

Clearly the boundary layers in CGILS and CGILS-like locations are different in all the configurations considered. In fact the differences in these clouds is much more than reported, for example there is increase in precipitation in CGILS-like locations in the coupled model, whereas the precipitation decreases in the amip model (Figure 3.10). The changes in precipitation in the deep convective regions is rather similar.

With these different boundary layer structure in CGILS-like location in amip and coupled model it is puzzling to see the changes in longwave cloud effects

### 3. LOW-CLOUD FEEDBACKS IN ECHAM6 AND CGILS FORCING

Table 3.3: Changes in 700hPa downward radiative fluxes ( $Wm^{-2}$ ) in amip configuration: downward longwave radiation (RLD), clear-sky downward longwave radiation (RLDCS), upward longwave radiation (RLU), clear-sky upward longwave radiation (RLD), downward shortwave radiation (RSD), clear-sky downward shortwave radiation (RSDCS), upward shortwave radiation (RSU), and clear-sky upward shortwave radiation (RSUCS)

<b>S11</b>	<b>RLD</b>	<b>RLDCS</b>	<b>RLU</b>	<b>RSUCS</b>
	37	35	-25	-23
	<b>RSD</b>	<b>RSDCS</b>	<b>RSU</b>	<b>RSUCS</b>
	-13	-6	10	1

in amip and coupled model are similar (Figure 3.3). The reason for this lies in changes in upper level relative humidity and associated changes in specific humidity. The changes in specific humidity can lead to increase in downwelling longwave radiation. Table 3.3 shows the components of downward radiative fluxes at 700hPa at amip S11 location. There is net increase of  $37 Wm^{-2}$  downward longwave radiation that compensates the increase in shortwave reflection. Due to limited model diagnostics, this cannot be verified in coupled configuration, although it is very likely the case. The increase in upper level humidity is likely due to changes in horizontal advection and lateral mixing. Increasing downwelling longwave can also stabilize the boundary layer but this doesnt appear to be valid here.

### 3.5 FORCING AND FEEDBACK MECHANISMS AT CGILS LOCATIONS

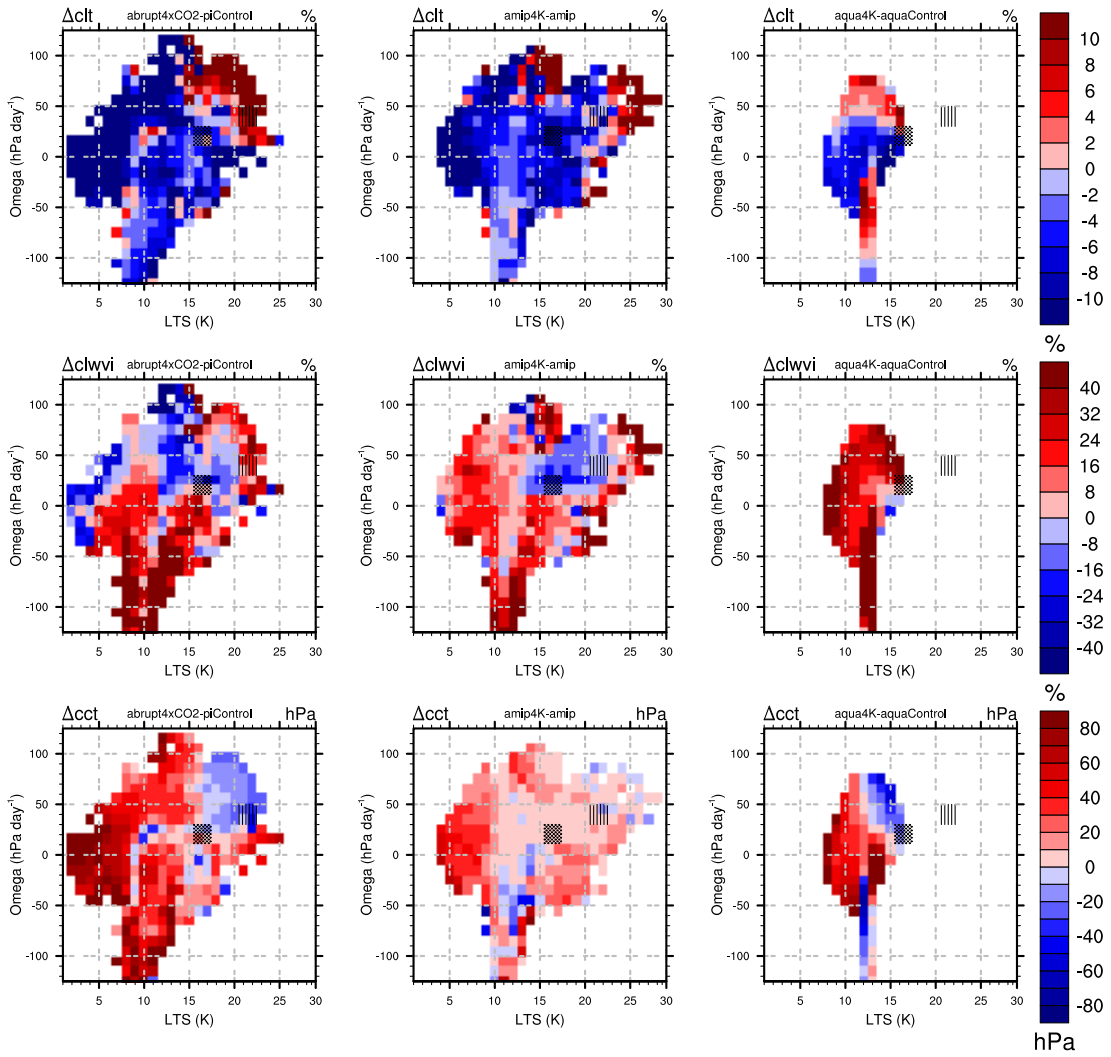


Figure 3.7: Percent changes in total cloud cover (upper) and liquid water path (middle) and absolute changes in cloud top height (hPa, bottom), in the GCM configurations. CGILS-like Stratocumulus and Shallow Cumulus regions are hatched with lines and dots.

### 3. LOW-CLOUD FEEDBACKS IN ECHAM6 AND CGILS FORCING

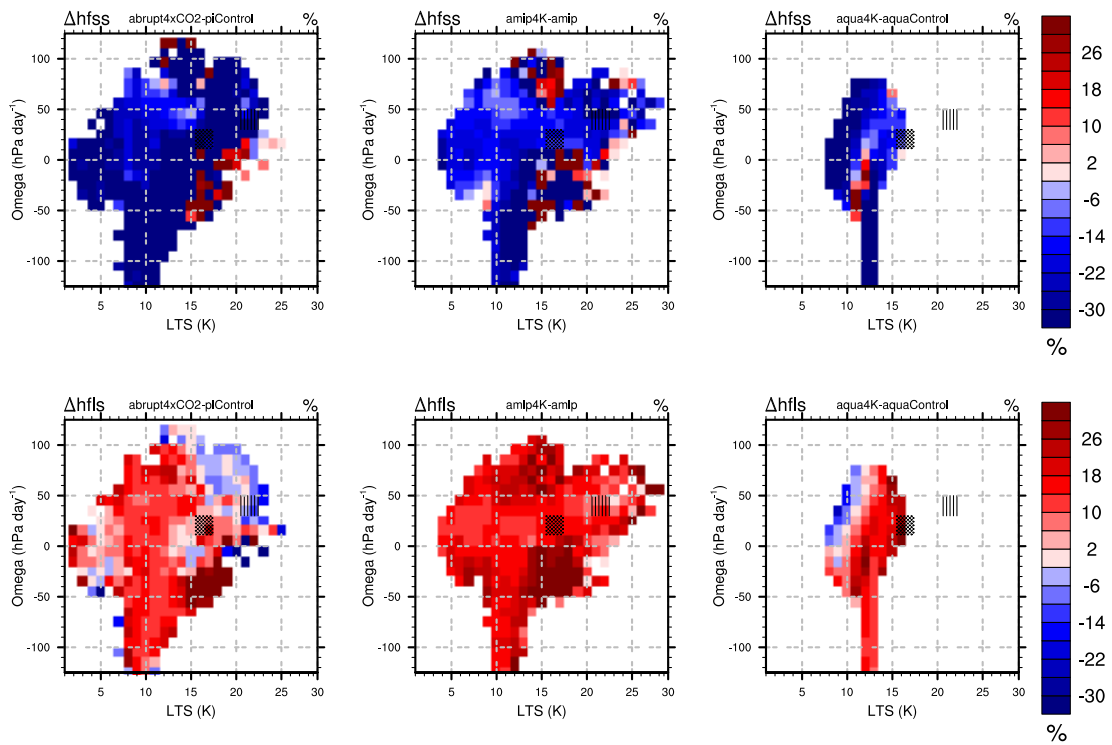


Figure 3.8: Percent changes in upward sensible heat flux (upper), upward latent heat flux (middle) in the selected GCM configurations. CGILS-like Stratocumulus and Shallow Cumulus regions are hatched with lines and dots.



### 3.5 FORCING AND FEEDBACK MECHANISMS AT CGILS LOCATIONS

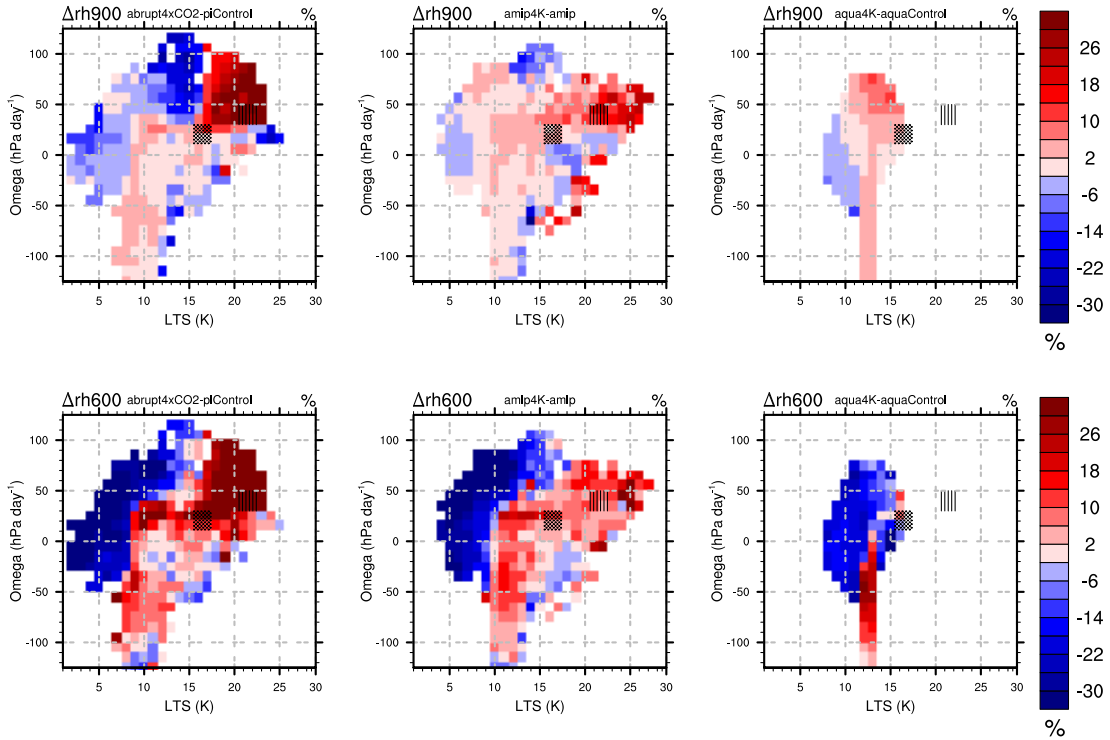


Figure 3.9: Percent changes in: vertical integrated relative humidity over 800hPa-1000hPa(upper); 500hPa-700hPa (bottom) .CGILS-like Stratocumulus and Shallow Cumulus regions are hatched with lines and dots.

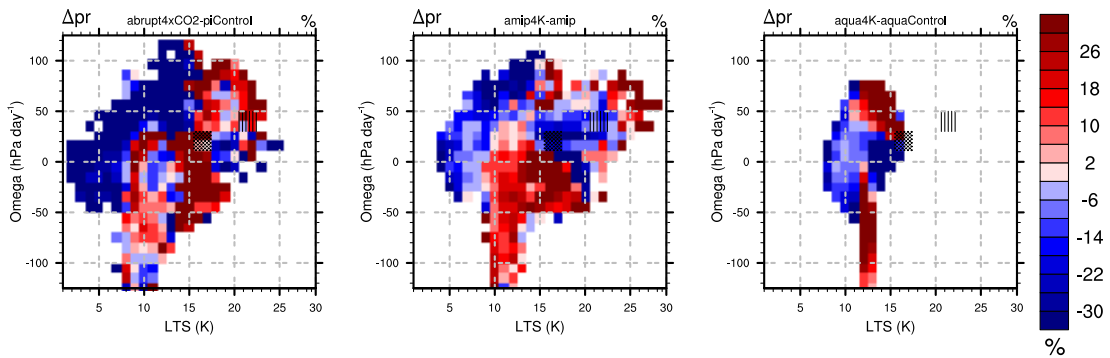


Figure 3.10: Percent changes in precipitation in selected heirarchy of GCMs.CGILS-like Stratocumulus and Shallow Cumulus regions are hatched with lines and dots.

### 3.6 Conclusions and Outlook

The response of tropical clouds is similar in MPI-ESM-LR amip and coupled model configurations. This similarity is mainly because amip model captures clouds in core distribution of the coupled model. There are substantial differences in boundary layer structure at CGILS and CGILS-like locations in the heirarchy of MPI-ESM-LR GCM configurations. But these regions do not contribute much to the tropical mean. Although the idealistic thermodynamic climate change captures certain aspects of changes in a coupled model, the deviations are significant. For example reduction in surface winds might be necessary to reproduce changes in BL structure of coupled model. It would be interesting to modify CGILS to incorporate changes in surface as seen in the coupled configuration. More valuable information can also be obtained from performing idealized sensitivity experiments to different aspects of large scale circulation eg. (Bellon and Stevens 2012).

It would be interesting to see the extent to which conclusions of this Chapter are valid for other models. In the next Chapter we explore if the responses of other single column models in CGILS are representative of changes in their coupled configurations.

# Chapter 4

## Low-cloud feedbacks in CMIP5 models and single column models in CGILS

### 4.1 Introduction

In Chapter 3, we compared in detail the cloud feedbacks across a hierarchy of MPI-ESM-LR model configurations. The goal of this chapter is to extend the comparison to the different models in CMIP5. This would help to draw conclusions about utility of CGILS idealized single column experiments to understand inter-model differences in low cloud feedbacks and additionally explore the representativeness of idealized large scale forcing to the projected changes in more comprehensive GCM configurations. The reasons why such comparison is interesting is described in Chapter 1 and Chapter 3.

Remainder of the Chapter is organized as follows. Section 4.2 provides an overview of all the models and their configurations used in the study. In Section 4.3 we examine ability of sorting method described in Chapter 3 to sort clouds in CMIP5 models. In Section 4.4 we present cloud feedbacks at CGILS and CGILS-like locations across the hierarchy of GCM configurations in CMIP5 and CGILS single column models. Section 4.5 we present representativeness of CGILS idealized forcing to that of changes projected in other GCM configurations. Conclusions and outlook from the chapter are presented in Section 4.6.

### 4.2 Overview of Cloud Feedbacks in the CMIP5 Models

Table 4.1 shows the models used in the study and symbols associated with them. There are 10 coupled models for which relevant experiments in amip configuration

#### 4. LOW-CLOUD FEEDBACKS IN CMIP5 MODELS AND SINGLE COLUMN MODELS IN CGILS

MODEL CENTER	SCM	COUPLED	AMIP	AQUA
CNRM-CERFACS	★	CNRM-CM5	★	CNRM-CM5
MOHC	✱ HadGEM2-A	✱ HadGEM2-ES	✱ HadGEM2-A	✱ HadGEM2-A
MPI	■ MPI-ESM-LR	■ MPI-ESM-LR	■ MPI-ESM-LR	■ MPI-ESM-LR
IPSL	♣ IPSL-CM5A-LR	♣ IPSL-CM5A-LR	♣ IPSL-CM5A-LR	♣ IPSL-CM5A-LR
		♣ IPSL-CM5B-LR	♣ IPSL-CM5B-LR	
MRI	¶ JMA	¶ MRI-CGCM3	¶ MRI-CGCM3	¶ MRI-CGCM3
MIROC	✱	MIROC5	✱ MIROC5	✱ MIROC5
NCAR	9 CAM4	9 CCSM4	9 CCSM4	9
MOHC	✱ HadGEM2-ES	✱ HadGEM2-ES	✱ HadGEM2-A	✱ HadGEM2-ES
LASG-CESS	ㄒ	FGOALS-g2	ㄒ FGOALS-g2	ㄒ FGOALS-g2

Figure 4.1: Table of CMIP5 models used

are available. There are 7 amip models for which aquaplanets configuration runs are also available. There are 15 single column models participating in CGILS intercomparison, out of which there are 5 models with outputs for both transient and constant large scale forcing.

Cess et al. 1990 proposed experiments using AMIPs with uniform increase in SST by 2K to understand the climate sensitivity of coupled models to doubling of CO<sub>2</sub>. They found that the climate sensitivity of majority of atmospheric models were similar to their coupled counterparts. With similar type of CMIP5 experiment pairs for amip and coupled but with much stronger perturbation we can see the extent to which this relation holds. Figure Figure 4.2 shows rank correlation of tropical cloud feedbacks (change in CRE per change in degree change in surface temperature) for amip and coupled configurations. A linear

### 4.3 SORTING CGILS CLOUDS

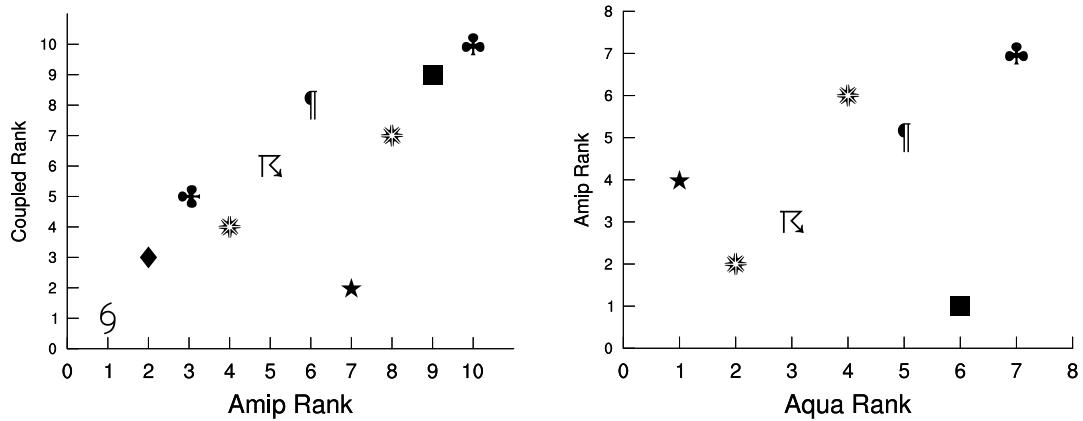


Figure 4.2: Rank correlation of tropical averaged CRE, for coupled models vs. amip models on the left and amip models vs. aquaplanets on the right.

correlation in the plot means that the differences between cloud feedbacks of different models is greater than the difference between the amip and coupled GCM configurations. An exception in this correlation is CNRM-CM5 model, it has a positive cloud feedback in the coupled configuration and a negative cloud feedback in amip configuration. This strong linear correlation would mean it is possible to use amip configurations to understand inter-model differences in cloud feedbacks of coupled configurations. This relation is not necessarily true for aquaplanets. the differences are most notable in MPI-ESM-LR and CNRM-CM5 models.

In the next section we would like to see the details to which these different configurations are similar, with more focus on cloud feedbacks at CGILS and CGILS-like locations.

### 4.3 Sorting CGILS Clouds

The rationale behind sorting is described in detail in Chapter 3. Figure 4.3 shows cloud top heights sorted using LTS and Omega for four CMIP5 models. It is clearly evident that LTS and Omega cleanly separate clouds into high clouds and low clouds. It is important to not that this clean separation would not be possible with using just Omega. Cloud top heights are similar in amip and coupled configurations. The cloud top height at S6-Like and S11-like locations are also well represented in models. An exception in the models is MRI-CGCM3 AMIP configuration. At the margins of stable regimes cloud top heights are much higher, often similar to convective regimes. These regions were mostly associated with coastal regions in this model.

The contour lines in the Figure 4.3 show joint distribution of occurrence of each

#### 4. LOW-CLOUD FEEDBACKS IN CMIP5 MODELS AND SINGLE COLUMN MODELS IN CGILS

regime. Cloud top height in the core regimes of amip and coupled configurations are similar. Aquaplanets tend to have bimodal distribution with more convective regimes. Cloud heights are higher in aquaplanets in general, similar to what was seen in chapter 2 for MPI-ESM-LR.

Figure 4.5 and Figure 4.6 show change in CRE sorted on LTS and Omega for the 7 models. The CGILS S11-like regions occur frequently at the margins of distributions. Figure 4.6 shows rank correlation of change in CRE at CGILS locations. Correlations in Figure 4.6 and Figure 4.3 suggests that the CGILS regions do not contribute much to inter-model differences in cloud feedbacks. Infact most regimes with cloud tops less than 1km do not contribute to inter-modal differences in cloud feedbacks.

### 4.3 SORTING CGILS CLOUDS

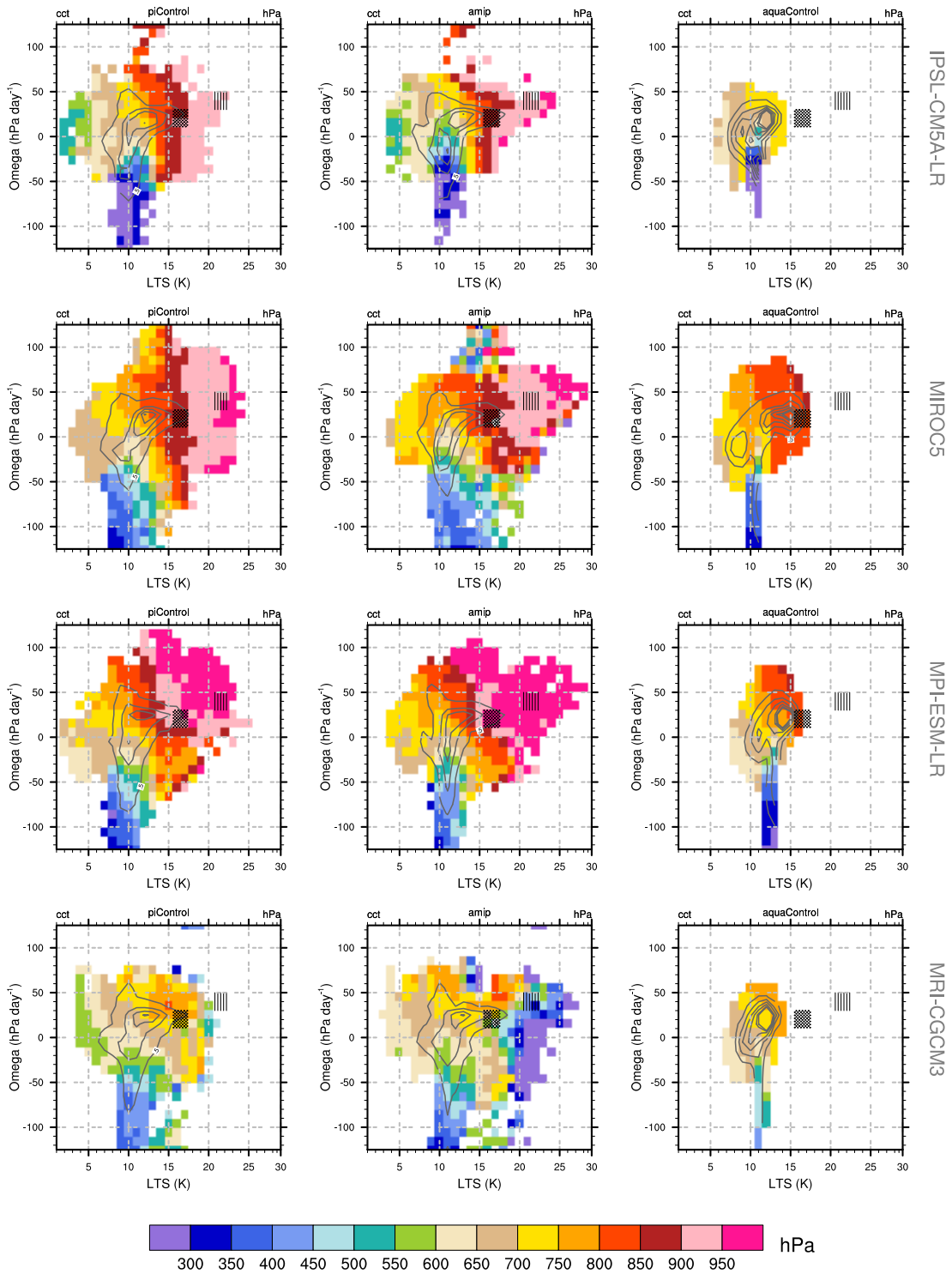


Figure 4.3: JJA average cloud top height (hPa) sorted based on omega at 500hPa and LTS. Joint distribution of omega and LTS are showed by black contour lines with 1% contour intervals. CGILS-like Stratocumulus and Shallow Cumulus locations, are indicated by shaded regions with lines and dots respectively.

#### 4. LOW-CLOUD FEEDBACKS IN CMIP5 MODELS AND SINGLE COLUMN MODELS IN CGILS

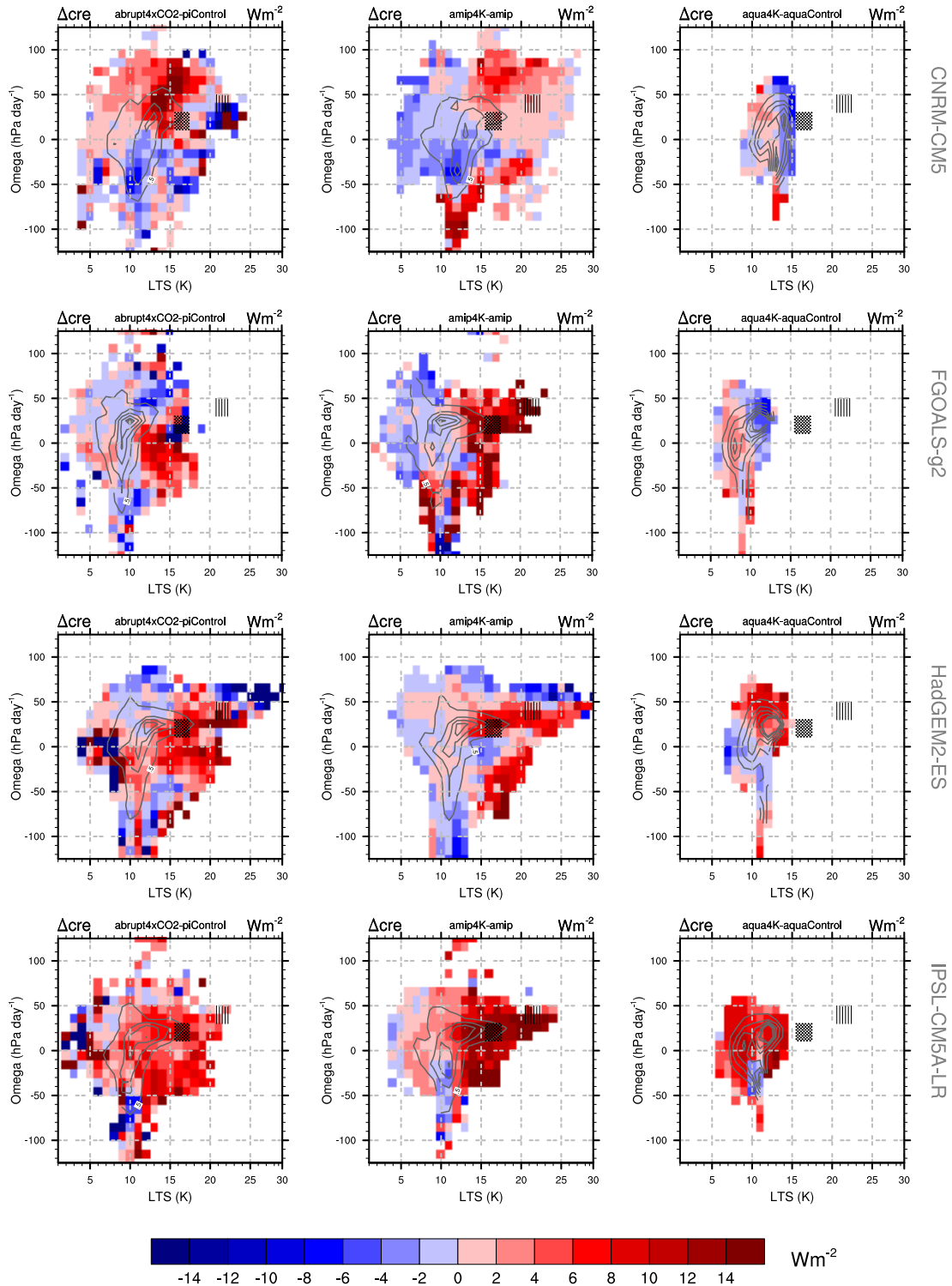


Figure 4.4: JJA average change in Cloud Radiative Effect ( $Wm^{-2}$ ) sorted on large scale vertical velocity and lower tropospheric stability. Joint distribution of omega and LTS are showed by black contour lines with 1% contour intervals. CGILS-like Stratocumulus and Shallow Cumulus locations, are indicated by shaded regions with lines and dots respectively.



### 4.3 SORTING CGILS CLOUDS

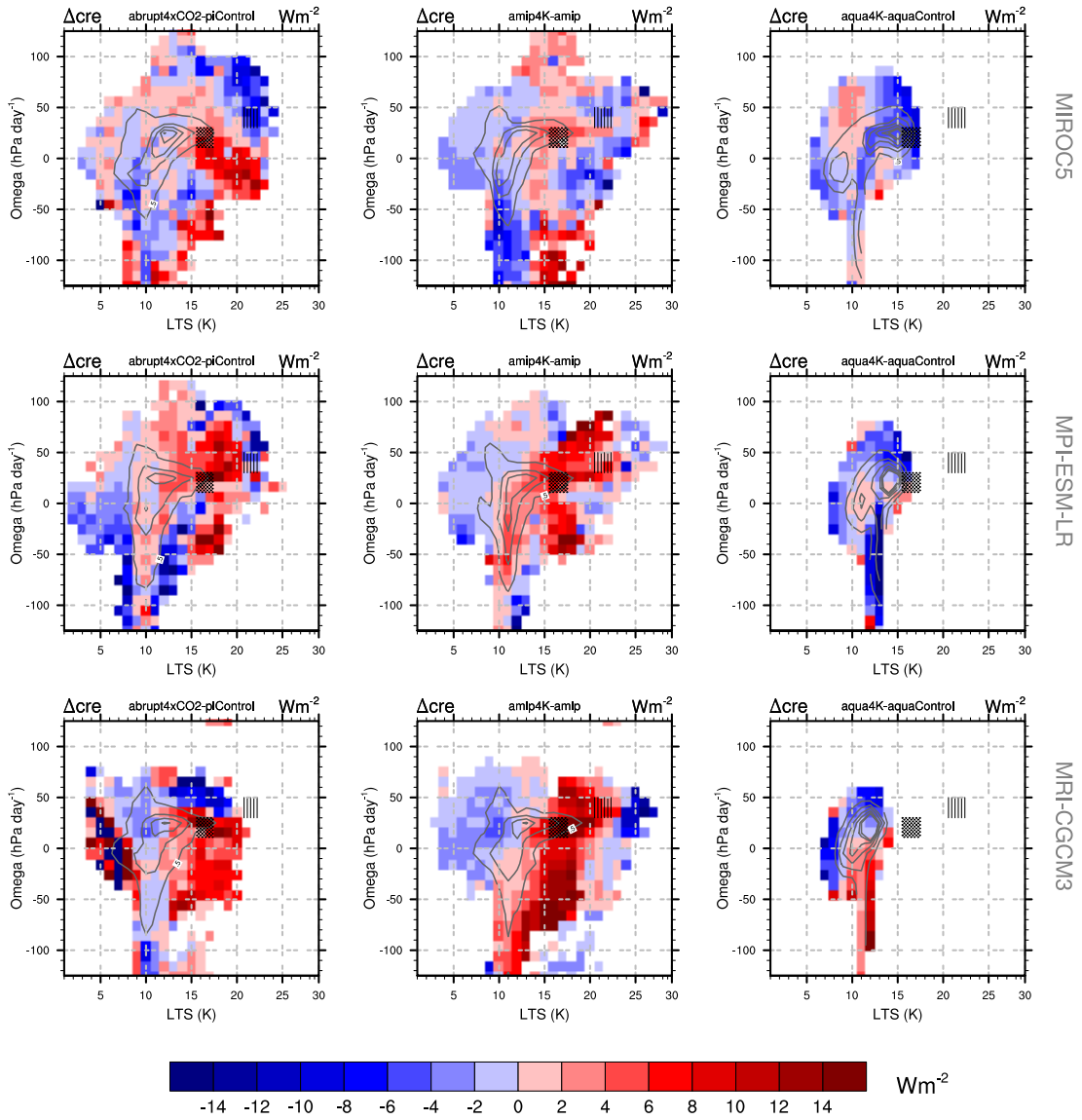


Figure 4.5: JJA average change in Cloud Radiative Effect ( $Wm^{-2}$ ) sorted on large scale vertical velocity and lower tropospheric stability. Joint distribution of omega and LTS are showed by black contour lines with 1% contour intervals. CGILS-like Stratocumulus and Shallow Cumulus locations, are indicated by shaded regions with lines and dots respectively.

#### 4. LOW-CLOUD FEEDBACKS IN CMIP5 MODELS AND SINGLE COLUMN MODELS IN CGILS

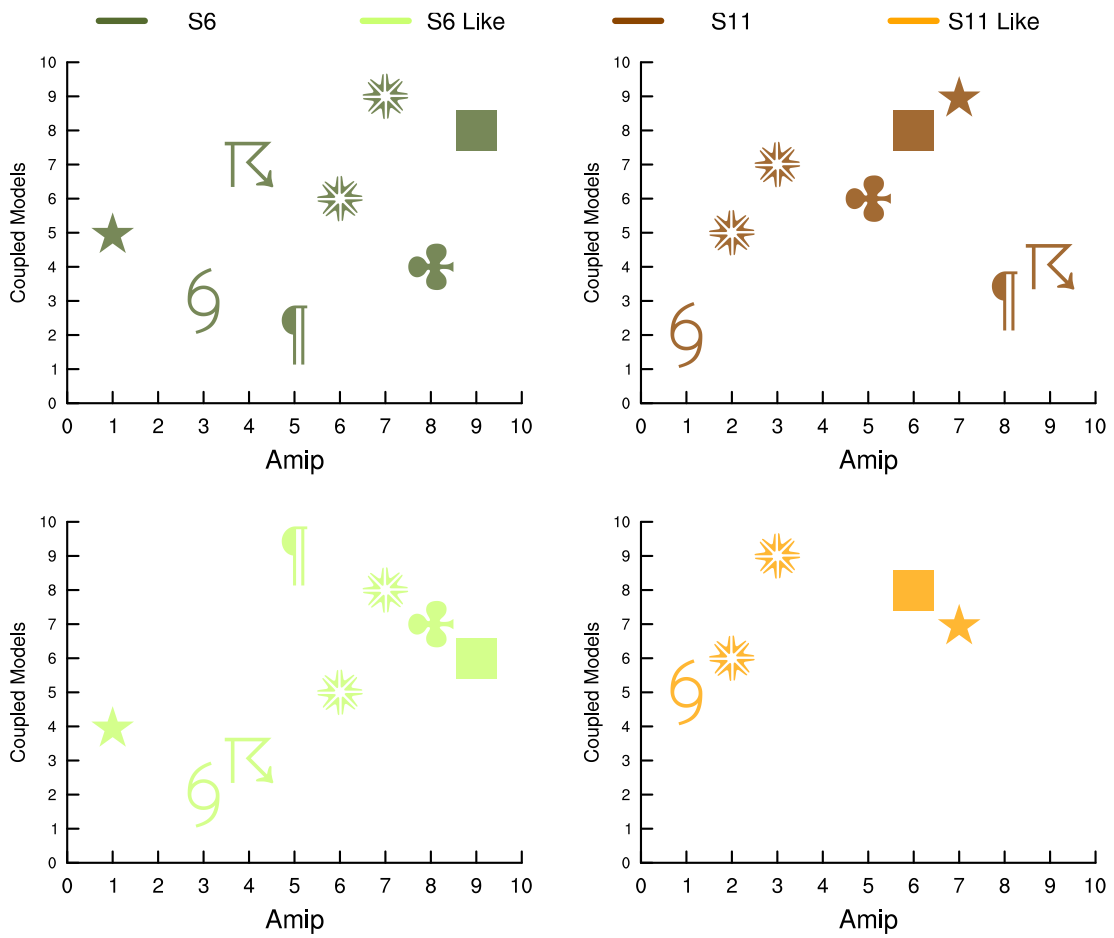


Figure 4.6: Rank correlation of CRE per degree of surface temperature change for coupled models vs. amip models.

## 4.4 Response in CGILS and CGILS-like areas

Figure 4.7 shows the range of cloud feedbacks across a hierarchy of GCM configurations for various models. The models in Single column model are from the CGILS intercomparison of single column models.

The interesting aspect here is the quartile range of CGILS cloud feedbacks using transient forcing is narrow than the one with Constant forcing. The tendency is to shift towards positive cloud feedbacks. It is interesting to note that despite being forced by same large forcing single column models exhibit wider range of solutions than their GCM counterparts.

The changes are mainly because of models which had less low cloud cover in constant forcing in control had more cloud cover control simulation of transient forcing. Other reasons for difference in behavior of single column models was described in Chapter 2.

Figure 4.8 shows rank correlation of cloud feedbacks from single column models and coupled models. Correlation is better at stratocumulus locations.

The arguments for designing changes in large scale environment at CGILS was described in Chapter 2 and Chapter 3. Figure 4.7 shows range of large scale environment at CGILS and CGILS-like regions. The range in coupled models is much more than other GCM configurations. Changes in LTS are stronger than CGILS in coupled and amip configurations. In contrary, changes in LTS are lower in the aquaplanets. Changes in HYL and Omega are similar across the model hierarchy. For the variables considered CGILS does capture some essential aspects of changes in large scale state of comprehensive models. Further analysis is required to asses details to which large scale changes are represented by CGILS.

#### 4. LOW-CLOUD FEEDBACKS IN CMIP5 MODELS AND SINGLE COLUMN MODELS IN CGILS

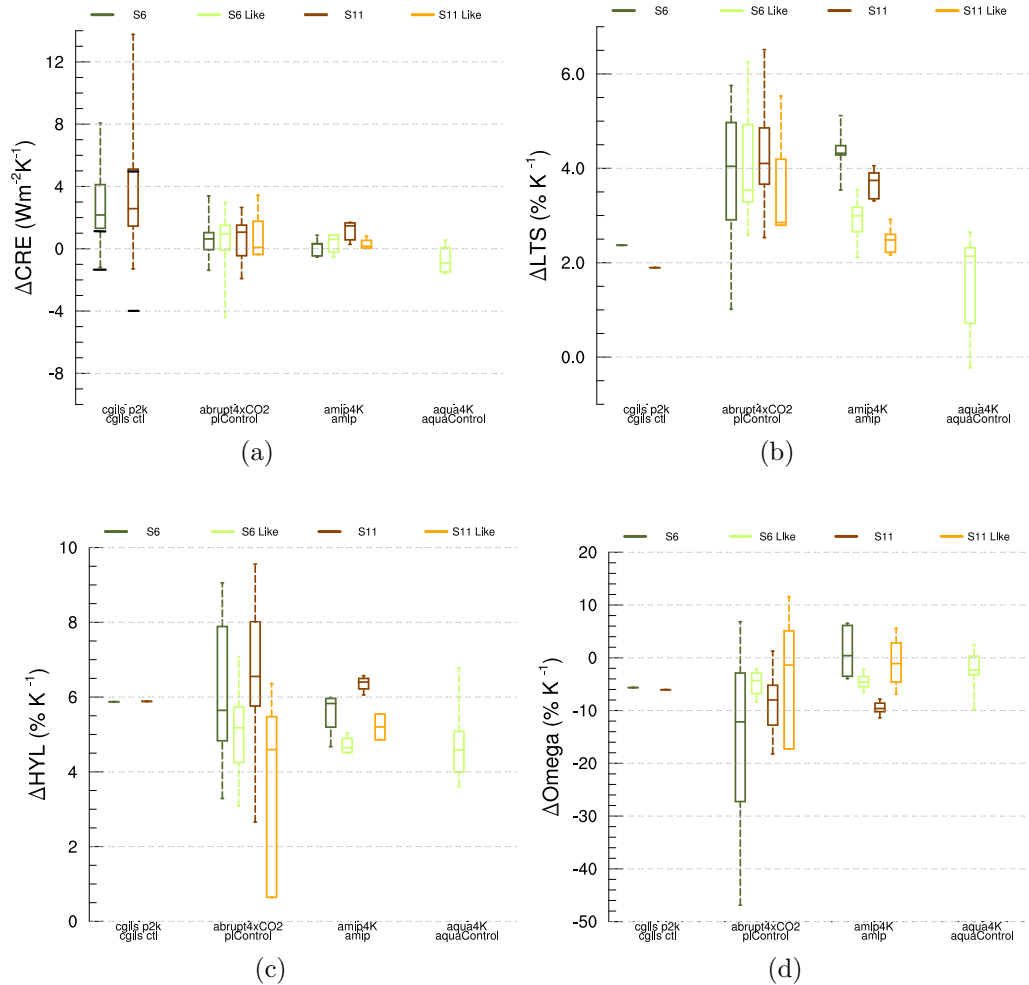


Figure 4.7: (a)Change in Cloud Radiative Effect( $Wm^{-2}$ ) b) Percentage change in LTS c) HYL and d) Omega at 500hPa, per degree of surface temperature change for CGILS and CGILS like locations. Quartile range from CGILS constant forcing is also indicated in Black

#### 4.4 RESPONSE IN CGILS AND CGILS-LIKE AREAS

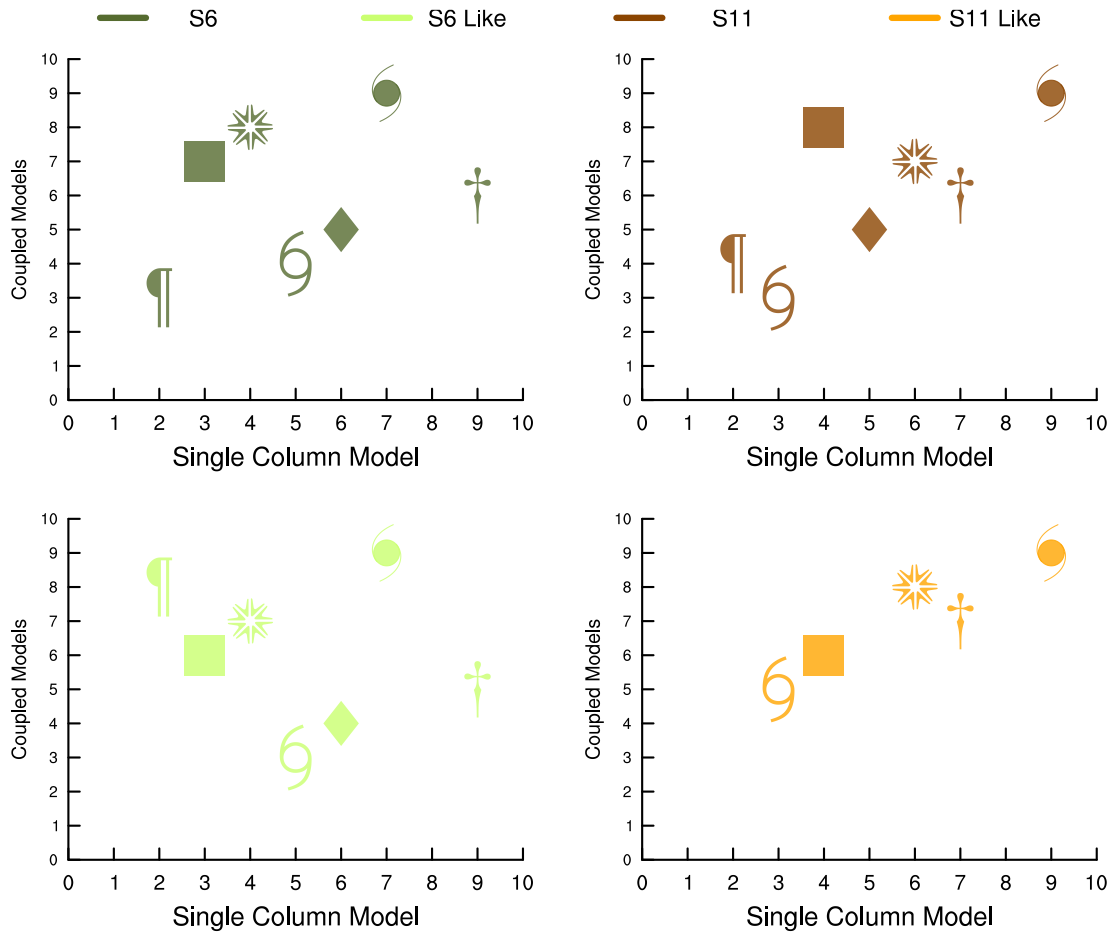


Figure 4.8: Rank correlation of CRE per degree of surface temperature change for coupled models vs. single column models.

## 4.5 Conclusions and Outlook

Single column models behave differently under transient largescale forcing. It is interesting to note that despite being forced by same large forcing single column models exhibit wider range of solutions than their GCM counterparts. This can be due to absence of largescale feedbacks in single column models. Conclusions from Chapter 3 based on MPI-ESM-LR are valid also for other CMIP5 models. More detailed analysis of changes in large scale state is desirable.

# Chapter 5

## Conclusions

In this Chapter we conclude the thesis by answering the objectives outlined in the Chapter 1.

- **To assess the ability of idealized single column model experiments to predict the low-cloud feedbacks in the GCMs.**

Various single column models from an intercomparison performing the same idealized experiments are compared to their comprehensive General Circulation Models (GCM) in CMIP5. We find that it is difficult to study inter-model differences in low-cloud feedbacks of GCMs using idealized test case for SCMs. The idealized low cloud regimes considered in the intercomparison occur at margins of distributions in most GCM configurations, hence they do not contribute much to the tropical average and hence any understanding from them is difficult to transfer to larger regions. We explored the representativeness of the changes in the large-scale environment used in the idealized test case of the SCMs to projected changes in the comprehensive GCM configurations. Although there are aspects of changes in large scale environment that are captured by the idealized test cases, the changes at the surface are not well represented. For instance in MPI-ESM-LR model configurations, we find that these changes at surface are possible reasons for the differences in cloud properties of the single column model and the comprehensive GCM configuration.

- **To evaluate CMIP5 models across the hierarchy of configurations to explore the robustness of cloud feedbacks.**

The study highlights use of heirarchy of GCM configurations to gain understanding of inter-model differences in low-cloud feedbacks. The tropical average cloud feedbacks in amip models are found to be similar to that of coupled models. This similarity is mainly because amip configurations capture the core of distribution of clouds in the coupled models. Use of amip configurations to study

## 5. CONCLUSIONS

other cloud regimes that are at margins of distributions are not necessarily representative. A related conclusion from the study is the regions of strongly stable and subsiding environment, such as stratocumulus and stratus regions do not contribute much to the inter-model differences in cloud feedbacks of the coupled configurations.

It might be hard to use aquaplanets to understand the inter-model differences in cloud feedbacks, in many models considered clouds in core distributions of aquaplanets do not necessarily correspond to that of coupled models.



# Bibliography

- Arakawa, A., 1975: *Modelling clouds and cloud processes for use in climate models*. 183–197 pp.
- Bellon, G. and B. Stevens, 2012: Using the Sensitivity of Large-Eddy Simulations to Evaluate Atmospheric Boundary Layer Models. *Journal of the Atmospheric Sciences*, **69** (5), 1582–1601, doi:10.1175/JAS-D-11-0160.1.
- Betts, A. and M. Miller, 1986: A new convective adjustment scheme. Part II: Single column tests using GATE wave, BOMEX, ATEX and arctic airmass data sets. *Quarterly Journal of the Royal . . .*, **112**, 693 –710.
- Bony, S., 2005: Marine boundary layer clouds at the heart of tropical cloud feedback uncertainties in climate models. *Geophysical Research Letters*, **32** (20), L20 806, doi:10.1029/2005GL023851.
- Bony, S., et al., 2006: How Well Do We Understand and Evaluate Climate Change Feedback Processes? *Journal of Climate*, **19** (15), 3445–3482, doi:10.1175/JCLI3819.1.
- Brient, F. and S. Bony, 2012: Interpretation of the positive low-cloud feedback predicted by a climate model under global warming. *Climate Dynamics*, **40** (9–10), 2415–2431, doi:10.1007/s00382-011-1279-7.
- Browning, K., G. Energy, W. Experiment, and G. C. S. S. Team, 1993: The GEWEX Cloud System Study (GCSS). *Bulletin of the American Meteorological Society*, **74** (3), 387–399.
- Gates, W. L., et al., 1999: An overview of the results of the Atmospheric Model Intercomparison Project (AMIP I). *Bulletin of the American Meteorological Society*, **80** (1), 29–55.
- Goswami, B. and J. Shukla, 1984: Quasi-periodic oscillations in a symmetric general circulation model. *Journal of the atmospheric sciences*, **40** (1), 20–37.
- Hack, J., J. Pedretti, and J. O. F. Climate, 2000: Assessment of Solution Uncertainties in Single-Column Modeling Frameworks. *Society*, **13** (2), 352–365.

## BIBLIOGRAPHY

- Hayashi, Y. and A. Sumi, 1986: The 30-40 day oscillations simulated in an "aqua planet" model. *J. Meteor. Soc. Japan*.
- Held, I. and B. Soden, 2000: Water Vapor Feedback and Global Warming 1. *Annual review of energy and the . . .*, **25 (1)**, 441–475.
- Held, I., B. Soden, N. Oceanic, and A. Science, 2006: Robust responses of the hydrological cycle to global warming. *Journal of Climate*, 5686–5699.
- Klein, S. A. and D. L. Hartmann, 1993: The Seasonal Cycle of Low Stratiform Clouds. *Journal of Climate*, **6 (8)**, 1587–1606, doi:10.1175/1520-0442(1993)006<1587:TSCOLS>2.0.CO;2.
- Larson, K., D. L. Hartmann, and S. A. Klein, 1999: The Role of Clouds, Water Vapor, Circulation, and Boundary Layer Structure in the Sensitivity of the Tropical Climate. *Journal of Climate*, **12 (8)**, 2359–2374.
- Medeiros, B. and B. Stevens, 2011: Revealing differences in GCM representations of low clouds. *Climate Dynamics*, **36 (1-2)**, 385–399, doi:10.1007/s00382-009-0694-5.
- Medeiros, B., B. Stevens, I. M. Held, M. Zhao, D. L. Williamson, J. G. Olson, and C. S. Bretherton, 2008: Aquaplanets, Climate Sensitivity, and Low Clouds. *Journal of Climate*, **21 (19)**, 4974–4991, doi:10.1175/2008JCLI1995.1.
- Miller, R. L., 1997: Tropical Thermostats and Low Cloud Cover. *Journal of Climate*, **10 (3)**, 409–440.
- Neale, R. and B. Hoskins, 2000: A standard test for AGCMs including their physical parametrizations: I: The proposal. *Atmospheric Science Letters*, **1 (2)**, 101–107.
- Pierrehumbert, R., 1995: Thermostats, radiator fins, and the local runaway greenhouse. *Journal of the atmospheric sciences*.
- Richter, I. and S.-P. Xie, 2008: Muted precipitation increase in global warming simulations: A surface evaporation perspective. *Journal of Geophysical Research*, **113 (D24)**, D24 118, doi:10.1029/2008JD010561.
- Rieck, M., L. Nuijens, and B. Stevens, 2012: Marine Boundary Layer Cloud Feedbacks in a Constant Relative Humidity Atmosphere. *Journal of the Atmospheric Sciences*, **69 (8)**, 2538–2550, doi:10.1175/JAS-D-11-0203.1.
- Soden, B., A. Broccoli, and R. Hemler, 2004: On the use of cloud forcing to estimate cloud feedback. *Journal of climate*, **17 (19)**, 3661–3665.

- Soden, B. and I. Held, 2006: An assessment of climate feedbacks in coupled ocean-atmosphere models. *Journal of Climate*, **19** (14), 3354–3360.
- Solomon, S., D. Qin, M. Manning, and R. Alley, 2007: *Climate change 2007: The physical science basis, contribution of working group 1 to the fourth assessment report of the Intergovernmental Panel on Climate Change*. 4th ed., Cambridge University Press.
- Stephens, G. L., 2005: Cloud Feedbacks in the Climate System: A Critical Review. *Journal of Climate*, **18** (2), 237–273, doi:10.1175/JCLI-3243.1.
- Taylor, K. E., R. J. Stouffer, and G. A. Meehl, 2012: An Overview of CMIP5 and the Experiment Design. *Bulletin of the American Meteorological Society*, **93** (4), 485–498, doi:10.1175/BAMS-D-11-00094.1.
- Teixeira, J., et al., 2011: Tropical and Subtropical Cloud Transitions in Weather and Climate Prediction Models: The GCSS/WGNE Pacific Cross-Section Intercomparison (GPCI). *Journal of Climate*, **24** (20), 5223–5256, doi:10.1175/2011JCLI3672.1.
- Vial, J., J.-l. D. Sandrine, J. Dufresne, and S. Bony, 2013: On the interpretation of inter-model spread in CMIP5 climate sensitivity estimates. *Climate Dynamics*, (Lmd), 1–22.
- Webb, M. J., et al., 2006: On the contribution of local feedback mechanisms to the range of climate sensitivity in two GCM ensembles. *Climate Dynamics*, **27** (1), 17–38, doi:10.1007/s00382-006-0111-2.
- Zhang, M. and C. Bretherton, 2008: Mechanisms of Low Cloud Climate Feedback in Idealized Single-Column Simulations with the Community Atmospheric Model, Version 3 (CAM3). *Journal of Climate*, **21** (18), 4859–4878, doi:10.1175/2008JCLI2237.1.
- Zhang, M., C. S. Bretherton, P. N. Blossey, S. Bony, F. Brient, and J.-C. Golaz, 2012: The CGILS experimental design to investigate low cloud feedbacks in general circulation models by using single-column and large-eddy simulation models. *Journal of Advances in Modeling Earth Systems*, **4**, M12001, doi:10.1029/2012MS000182.
- Zhang, Y., B. Stevens, B. Medeiros, and M. Ghil, 2009: Low-Cloud Fraction, Lower-Tropospheric Stability, and Large-Scale Divergence. *Journal of Climate*, **22** (18), 4827–4844, doi:10.1175/2009JCLI2891.1.

# Acknowledgments

I would like to thank Bjorn Stevens for being my adviser, and introducing me to this fascinating world of low clouds. He has inspired me in more ways than his lightning speed of thought and passion towards science. Working with him, I also learnt to be more independent, and balance the excitement from the new ideas vs. focusing on things we started. I am greatly indebted to him for introducing me to the boundary layer community. The people from GCSS boundary layer community have induced some of their passion towards atmospheric boundary layer in me, at-least to an extent that it will remain my permanent area of interest. Marco's in-depth knowledge of the ECHAM model always pushed me to further explore the code with excitement, which otherwise could have been frustrating. Long discussions with Anurag and Eckhard on numerics were fun and gave me valuable insight into ways of controlling numerical errors. I benefited a lot from numerous discussions from the atmosphere department colleagues of the MPI. Louise, Johannes Quass, Thijs, Christine Nam, Katrin, Anurag, Eleftheria, Gilles, Robert Pincus, Heiko, Juan Pedro, Benjamin, Max, Irina Sandu and Vera gave me a valuable advice and feedback on my work during the times of stress.

My thesis wouldn't be possible without support from Antje, Jochem, and Andreas Chlond. I adore Antje for being one of the nicest people I know and for making the PhD school, the IMPRS, the way it is. Conni and Wiebke provided extraordinary support for all the bureaucratic things needed for my living and the thesis. Angela provided all possible support through out my PhD, without which I probably would have taken much longer to finish my thesis. Administration and IT at the MPI were always very friendly. Ever positive Bettina helped me print many posters in nick of time.

The students from IMPRS were always fun to hangout with. My time with Freja, Florian, Christina, Doerte, Jan, Josiane, Daniel Klocke, Thomas Keitzl, Francesco, Werner, Rosy, Thomas Raub, Torsten, Steffen, Seethala, Laura, Sebastian, Antonija and Philipp and the days at the IMPRS and Institute retreats are memorable. Friends like Armelle, Natasha, Swantje, Stergios, Dimitris, Irini, Nasia, Katrin, Louise, Gabi and Vera prove a point that like-minded people exist cutting across cultures and borders, I thank them for the great time we had and bearing with my complaints. Holidays with Olga and Thomas have charged me

## BIBLIOGRAPHY

after a burn-out. After-office beer with Vera was sometimes the only thing I was looking forward to in the day.

Despite my resistance to form a group of Indian friends, I landed up making many good friends, with-whom I cannot avoid being sarcastic. I thank Anurag for promising to play table tennis and badminton with me; Ashu for teaching me how to speak perfect Hindi; Rittik for his tips on body-building, which somehow worked only on him; Pankaj ji and Seshu for their insight on Indian monsoon; Ketan for convincing me to smoke an electronic cigarette; Kamesh for pursuing me to vote for his political party; Pavan for sharing his insight on data security and privacy; Hanna, Swathi and Bipin for inviting me home at the times when I was craving for the Indian food; Rohit and Seshu for the numerous dinners we shared and teaching me how to cook hours to make a perfect meal.

I thank Eleftheria for being by my-side almost thought my time in Hamburg. She stole my time during stressful days and most of my little holidays of the year, and further imposed her political ideology on me. She trained me to focus faster by fighting with me at wrong times.

I am greatly indebted to my parents for all the freedom and unconditional support they gave throughout my life. Their high regard for education is probably why I have pursued a PhD. The moral values set by my grandparents will always remain my reference. The support and encouragement from my sister Aparna and brother-in-law, Sushobith has always pushed me to take one extra step. My unending list of cousins, aunts and uncles have encouraged and instilled some self confidence in me.

I dedicate all my endeavors to all the ancestors of homo sapiens for the struggle they put up for millions of years to provide me this lucky opportunity to live.

## **Eidesstattliche Erklärung**

Hiermit versichere ich, dass ich diese Dissertation selbständig verfasst habe und keine anderen als die angegebenen Quellen und Hilfsmittel benutzt habe.

Suvarchal Kumar Cheedela,  
Hamburg, den 15 May 2013